Y-DR-44

STATIC AND DYNAMIC EXPERIMENTS WITH A REPETITIVELY PULSED BOOSTER

J. T. Mihalczo

UNION CARBIDE CORPORATION
NUCLEAR DIVISION
OAK RIDGE Y-12 PLANT

operated for the ATOMIC ENERGY COMMISSION *under* U. S. GOVERNMENT Contract W-7405 eng 26

OAK RIDGE Y-12 PLANT
P. O. Box Y
OAK RIDGE, TENNESSEE 37830

DISCLAIMER

Date Issued: March 22, 1971 Report Number: Y-DR-44

UNION CARBIDE CORPORATION
Nuclear Division

Oak Ridge Y-12 Plant

Contract W-7405-eng-26
With the U.S. Atomic Energy Commission

STATIC AND DYNAMIC EXPERIMENTS WITH A REPETITIVELY PULSED BOOSTER

J. T. Mihalczo

Oak Ridge, Tennessee

CONTENTS

LIST OF FIGURES

STATIC AND DYNAMIC EXPERIMENTS WITH A REPETITIVELY PULSED BOOSTER

John T. Mihalczo

ABSTRACT

A series of dynamic measurements have been performed with a multiplying assembly in which a rotating beryllium reflector (worth 4.8 dollars in reactivity) moved past an unreflected core surface ~60 times/sec at a speed of 264 meters/sec. A pulse of 14.1 MeV neutrons (~1 μsec wide) was injected into the assembly each time the rotating reflector attained a position for which the reactivity of the assembly was maximum. The time distribution of neutrons after injection of the pulse was measured. The maximum prompt neutron multiplication of the assembly, which was reflected with iron on all sides but one and contained 58.6 kg of uranium (enriched to 93.2 wt % in ^{235}U isotope) metal at delayed criticality, was varied by fuel loading changes from 75 to 285.

The pulsed assembly, with a maximum prompt neutron multiplication of 285, produced neutron pulses having a width at half maximum of 3.9 μsec and a peak-to-minimum ratio of 12,400. The pulse, when thermalized by a 10.16 x 10.16 x 3.81 cm polyethylene scatterer, was broadened to a width at half maximum of 20.9 μsec with a peak-to-minimum ratio of 1590. The use of cadmium in the scatterer can neither reduce the width of the pulse of neutrons to less than 7 μsec nor increase the peak-to-minimum ratio to more than 7400. The fraction of all neutrons that are in the pulse varied with reactivity and the position of the measurement from 0.77 to 0.85.

The number of thermal neutrons leaking from the outer surface of the scatterer was 3.3×10^{-5} n/cm^2-fission. Thus, a repetitively pulsed booster of this type with 1/60 MW-sec of energy in the pulse would produce a leakage fluence of $\sim 1.7 \times 10^{10}$ thermal neutrons/cm^2 per pulse.

INTRODUCTION

Repetitively pulsed reactors are useful for experiments that require very high neutron fluxes for very short times. Instantaneous neutron fluxes hundreds of times larger than average can be obtained by periodically varying the reactivity through prompt criticality. The IBR Reactor[1] at Dubna, Russia, has been in operation since 1960 at average powers of up to 6 kW. Another repetitively pulsed reactor, EBER II, with an average power of ~5 MW is being built at Dubna for operation about 1975.[2] Design studies for this type of reactor with an average power of ~1 MW[3] were started by EURATOM at Ispra in 1962. However this reactor differed from the IBR in that the rotation of reflector material adjacent to the core rather than motion of fissile material through the core produced the reactivity variation. Several laboratories in this country have considered the procurement of repetitively pulsed reactors. One of these systems was proposed by Brookhaven National Laboratory.[4,5] Others such as Idaho Nuclear Corporation[6] and Los Alamos Scientific Laboratory[7] investigated the use of such a reactor. Oak Ridge National Laboratory (ORNL) has considered the possible use of this type of reactor.[8]

1. G.E. Blokhin et al., "A Fast Neutron Pulse Reactor," translated from Atomnayia Energiya, Vol. 10, No. 5, pp. 437-446 (1961).
2. V. D. Anan'cu et al., "The Operational Experience and Development of Periodically Pulsed Reactors at Dubna," Proc. of Seminar on Fast Burst Reactors, Albuquerque, New Mexico (1969); The USSR Nuclear Power Program: Report of the U.S. Reactor Delegation, Nuclear News 13, No. 10, p. 21 (1970).
3. J. A. Larrimore et al., "The SORA Reactor," Proc. of a Seminar on Intense Neutron Sources, Santa Fe, New Mexico, September 1966, CONF-660925, p. 373 (1967).
4. K. C. Hoffman et al., "Engineering Problems in Pulsed Neutron Sources," Proc. of a Seminar on Intense Neutron Sources, Santa Fe, New Mexico, September 1966, CONF-660925, p. 509 (1967).
5. Fundamental Nuclear Energy Research, 1967 Supplemental Report to the Annual Report to Congress for 1967 of the United States Atomic Energy Commission, p. 176 (1968).
6. R. G. Fluharty et al., "A Proposal for a Repetitively Pulsed Test Facility (RPTF)," IN-1149, Idaho Nuclear Corporation (1967).
7. R. G. Fluharty, "Short Moderator Pulses and Booster Systems," Proc. of a Seminar on Fast Burst Reactors, Albuquerque, New Mexico, January 1969 (1969).
8. Memo to S. E. Beall from W. K. Ergen, "High Flux Reactor Study," (Aug. 21, 1967); Memo to A. D. Callihan from F. C. Maienschein, (Sept. 19, 1967).

Repetitively pulsed boosters for accelerators have been operated[9] and have been under study[7,10] as a means of producing narrower pulses than repetitively pulsed reactors. In the booster concept the reactor near delayed criticality multiplies neutrons produced by an accelerator. Decreasing the reactivity between pulses by removal of reflector or fissile material lowers the background between pulses.

A program of static critical experiments in support of the final design of the EURATOM reactor (SORA) was performed at ORNL from Sept. 1965 to Aug. 1966 under a cooperative agreement between EURATOM and the United States Atomic Energy Commission. These experiments were performed with a mockup of the SORA reactor differing from the reactor design principally in the use of iron in the core in place of the liquid metal coolant, of iron as the reflector material instead of tungsten or molybdenum, and the use of uranium as the fuel in place of a uranium-molybdenum alloy. Measurements of the prompt neutron decay constant, fission rate distributions, control rod calibrations, temperature coefficient of reactivity, material replacements in the core, reactivity of simulated movable reflectors, and of the reactivity effects of the parts of the fixed reflector were performed. These results have been described previously.[11]

Based on information obtained in these static experiments, the experimental assembly was modified to include a rotating reflector which moved by the unreflected core surface ~60 times/sec with a speed of 264 meters/sec. After measurements of the static properties of the assemblies, repetitively pulsed experiments were performed to obtain the pulse characteristic of the assembly.

---

9. L. B. Pikelner and V. T. Rudenk, "IBR Pulsed Reactor with Injector," Proc. of a Panel on Research Applications of Nuclear Pulsed Systems, Dubna, p. 165 (1966).
10. J. R. Beyster and C. A. Stevens, "Feasibility Study of an Accelerator-Booster, Fast, Pulsed Research Reactor," GA-7381, General Atomic (1966); M. J. Poole, "The Superbooster," Proc. of a Seminar on Intense Neutron Sources, Santa Fe, New Mexico, September 1966, CONF-660925, p. 431 (1967).
11. G. Kistner and J. T. Mihalczo, Nucl. Sci. Eng. 35, 27 (1969).

Because the maximum reactivity was 50 cents above delayed criticality, the results of these experiments are more useful for the design of a repetitively pulsed booster for an accelerator rather than for a repetitively pulsed reactor in which the reactivity is in excess of prompt criticality. These experiments also provided information which can be used to determine the validity of the methods of predicting the results of kinetic experiments from parameters measured in static experiments.

Withdrawal of support for this work resulted in premature termination of these experiments and minimal interpretation of the data.

DESCRIPTION OF THE ASSEMBLY

The assembly consisted of three major parts, a core composed of uranium metal distributed in iron, a fixed iron reflector which contained the polyethylene scatterer, and a rotor assembly which moved the reflector past the otherwise unreflected core face. The experiments were performed with a vertical assembly machine previously described by Rohrer et al.[12]

The core consisted of a 31.6-cm-long iron matrix containing 1.379-cm-diam uranium metal rods (93.18 wt % ^{235}U, ρ = 18.75 g/cm^3). The uranium was 24 cm in height and the top of the uranium rods was 0.25 cm below the top of the iron matrix. The space below the uranium was filled with 1.369-cm-diam iron rods. A cross section of a typical core is shown in Fig. 1. The reactivity in these experiments was varied by changes in the core loadings as described in Appendix A. The mass of uranium in the core varied from ~49 to ~59 kg. Three thermocouples were provided in one of the central fuel rods (No. 60), one at the center of the rod, and the other two ~1.2 cm from each end. The core was mounted on a 10-cm-thick piece of iron which had the same hexagonal cross sectional dimensions as the core matrix. This plate together with the lower section of the core matrix which contained iron rods served as the 17.6-cm-thick bottom reflector. The core and bottom reflector were mounted on the vertical lift of the assembly machine.

The side pieces of the fixed reflector consisted of 48.0-cm-high iron and beryllium blocks with various cross sectional shapes as shown in Fig. 2. The beryllium was adjacent to the unreflected core surface. A considerable amount of the 29-cm-thick side reflector of the previous experiment[11] had been removed so that the prompt neutron lifetime in this assembly would be shorter. A 10.16 x 10.16 x 3.81 cm block of polyethylene (ρ = 0.92 g/cm^3) at room temperature (20°C) was used as the

---

12. E. R. Rohrer et al., Neutron Phys. Div. Ann. Prog. Rept. Sept. 1, 1961, ORNL-3193, Oak Ridge National Laboratory, p. 168 (1961).

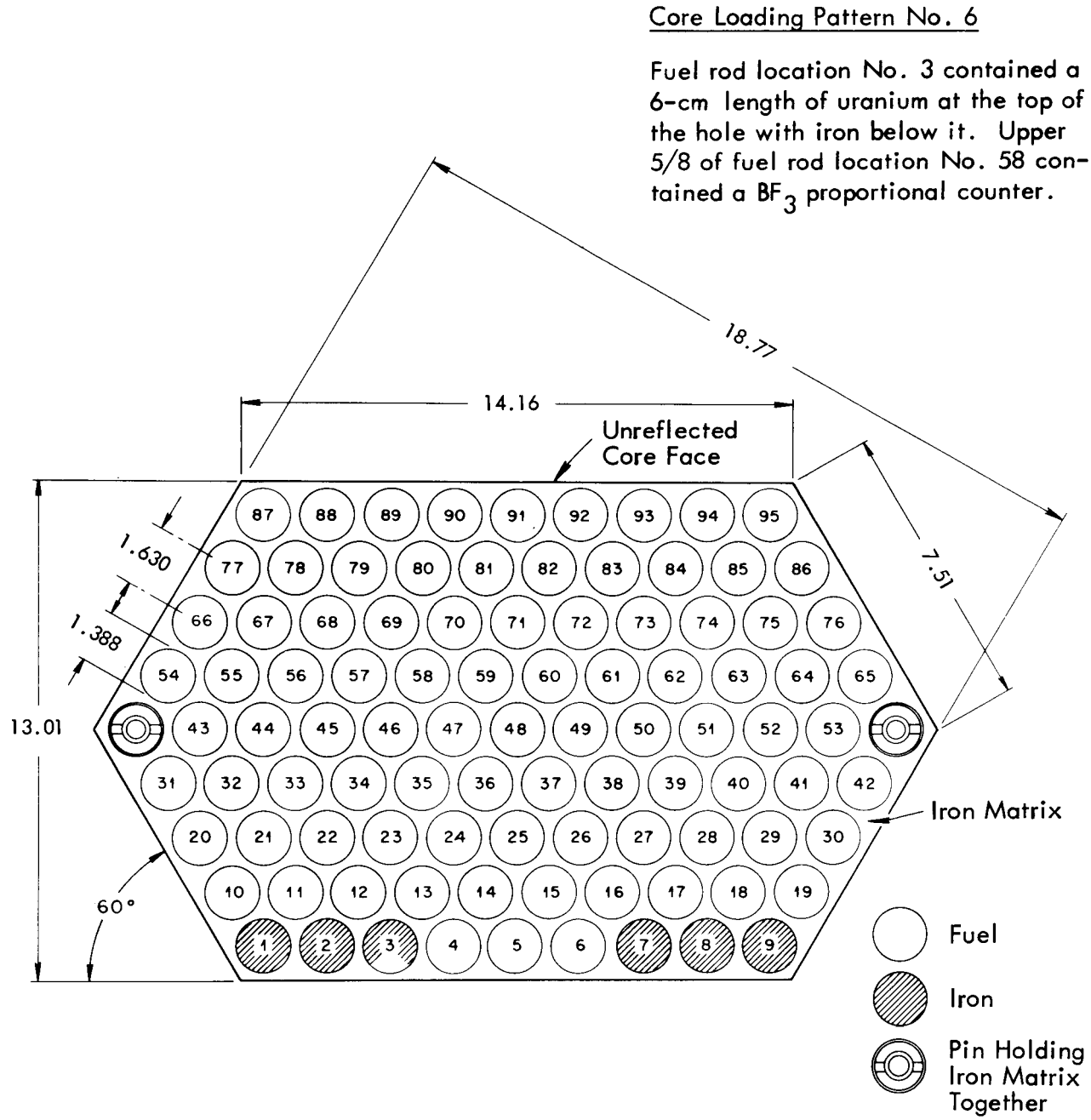

Fig. 1. Horizontal Section Through a Core Assembly Identifying the Fuel Rod Locations. (All Dimensions in Centimeters)

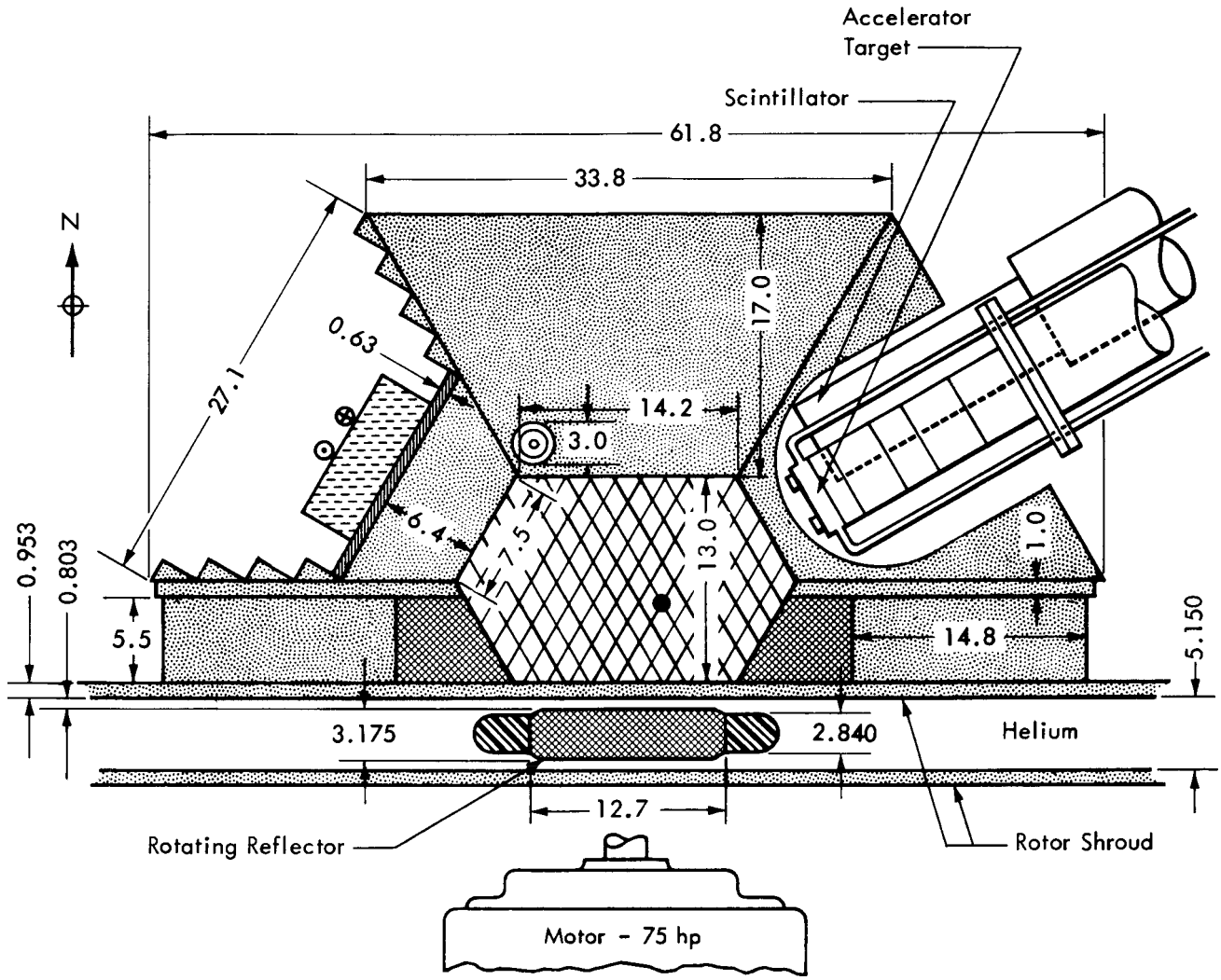

Core Matrix (fuel rod locations centered at crosses)

Beryllium

Iron

Boron Carbide Canned in Aluminum (Boral)

Polyethylene (10.16 x 10.16 x 3.81, cadmium covered except side facing core)

Titanium Alloy

2.54-cm-diam, 20.64-cm-long BF_3 Proportional Counter

0.79-cm-diam, 2.54-cm-long BF_3 Proportional Counter in Fuel Rod Location No. 58

0.79-cm-diam, 2.54-cm-long BF_3 Proportional Counter Covered with 0.064-cm-Thick Cadmium

0.79-cm-diam, 2.54-cm-long BF_3 Proportional Counter

The scintillator (5.1-cm-diam, 1.27-cm-long) was located with its axis in a plane 5.5 cm below the horizontal midplane.

Fig. 2. Cross Section of the Assembly at the Horizontal Midplane of the Core. (All Dimensions in Centimeters)

scatterer to thermalize the fast neutrons leaking from the core.[13] The polyethylene was covered with 0.063-cm-thick cadmium except for the 10.16 x 10.16 cm vertical surface nearest the core which was adjacent to a 0.63-cm-thick Boral plate (0.33 g of boron/cm^2). The Boral plate decoupled the thermal neutrons of the scatterer from the core. This size scatterer instead of the much larger scatterers of the SORA design was chosen because of the expected narrow width of the incident pulse from the core of the assembly. This narrow pulse width was a result of the reactivity being 50 cents or more below prompt criticality in these repetitively pulsed experiments.

The target assembly of the Cockcroft-Walton accelerator was located in the side reflector 4 cm from the core surface. The center of the target assembly was in a horizontal plane through the core center. A 17-cm-thick iron top reflector had the same hexagonal cross section as the core matrix. This reflector contained three vertical penetrations: a 0.95-cm-square hole for BF_3 counter cables above fuel rod location No. 58 in the core matrix, a 1.27-cm-diam hole for thermocouple wires above fuel rod location No. 60, and a 5.72-cm-diam hole centered above fuel rod location No. 28 which could accomodate a 5.1-cm-diam proton recoil scintillation counter. A sketch of the top reflector is shown in Fig. 3.

A 176-cm-diam iron shroud was mounted on the unreflected side of the core. This shroud enclosed the rotor which contained the movable beryllium reflector. Copper tubing, soldered to the periphery of the shroud, provided water coolant to remove the heat generated in the gas within the shroud by rotor friction. The movable beryllium reflector was mounted in a titanium-aluminum-vanadium alloy blade which rotated within this shroud in a helium atmosphere slightly above ambient pressure. The dimensions of the beryllium reflector were 21.91 x 12.70 x 3.175 cm and its center rotated with a speed of 264 meters/sec. A drawing of the blade is shown in Fig. 4. The blade was mounted on a

---

13. R. G. Fluharty, F. B. Simpson, G. J. Russell, and J. H. Menzel, Nucl. Sci. Eng. 35, 45 (1969).

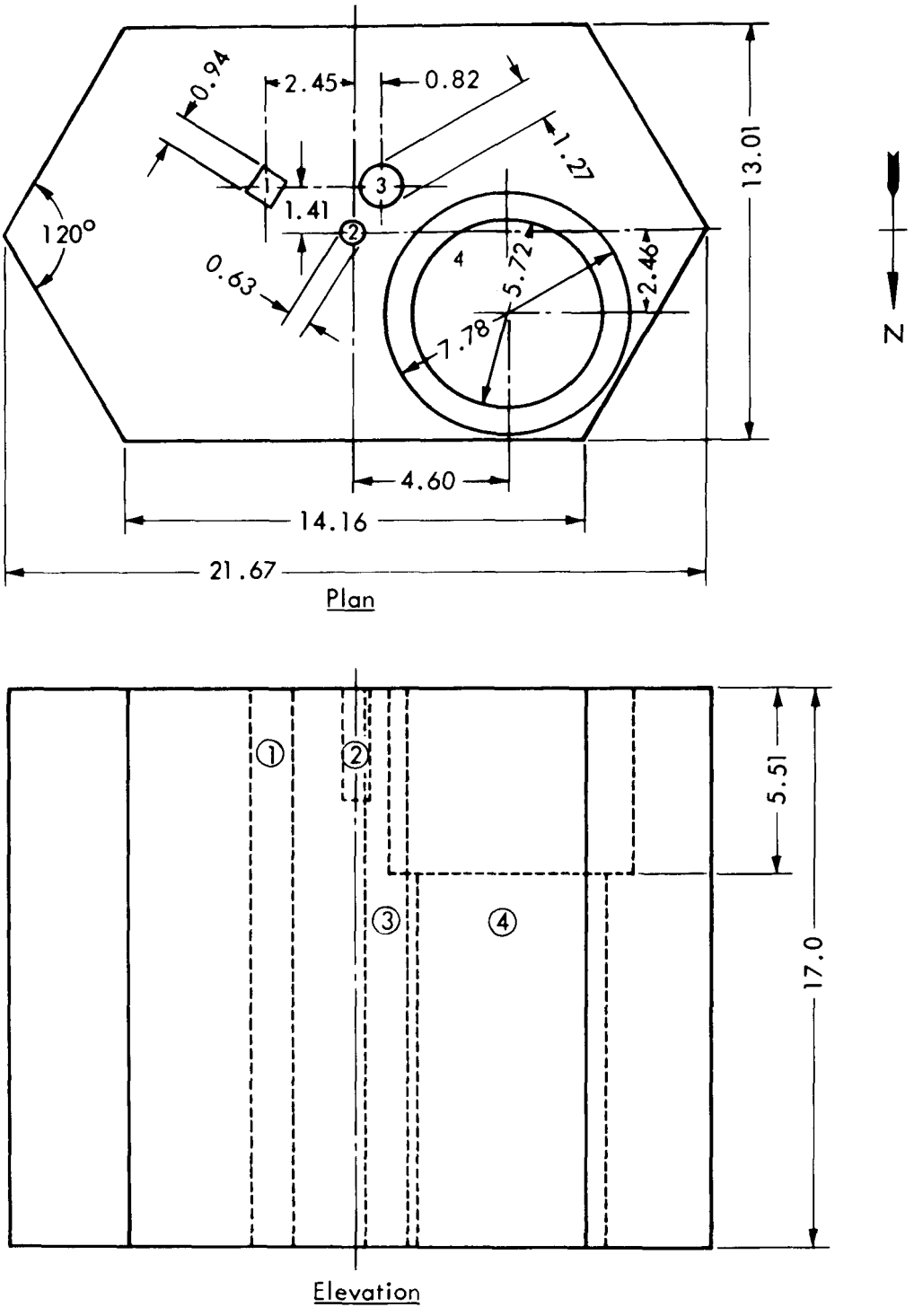

① Hole for BF_3 Counter Cables above Fuel Rod Location No. 58 (see Fig. 1)
② Tapped Hole for Eye Bolt
③ Hole for Thermocouple Wires above Fuel Rod Location No. 60 (see Fig. 1)
④ Hole to Accommodate 5.1-cm-diam Plastic Scintillator, Photomultiplier, and Base

Fig. 3. Sketch of Top Reflector. (All Dimensions in Centimeters)

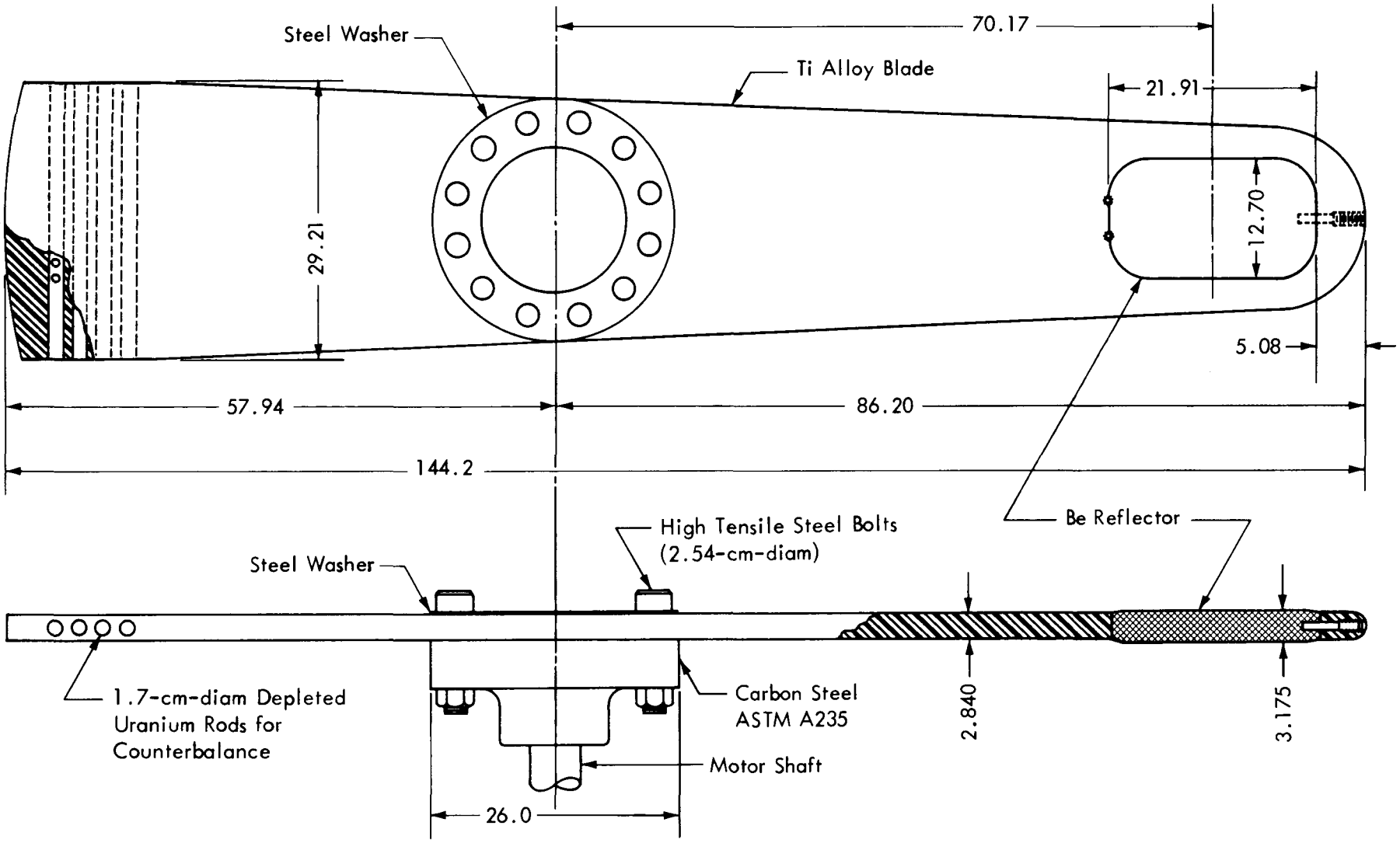

Fig. 4. Rotor Detail. (All Dimensions in Centimeters)

hub, also shown in Fig. 4, which was attached directly to the shaft of a 75 hp synchronous motor. A pictorial sketch of the assembly is shown in Fig. 5. Some results of the mechanical tests with the rotating assembly and the results of examinations of the rotor are given in Appendix B.

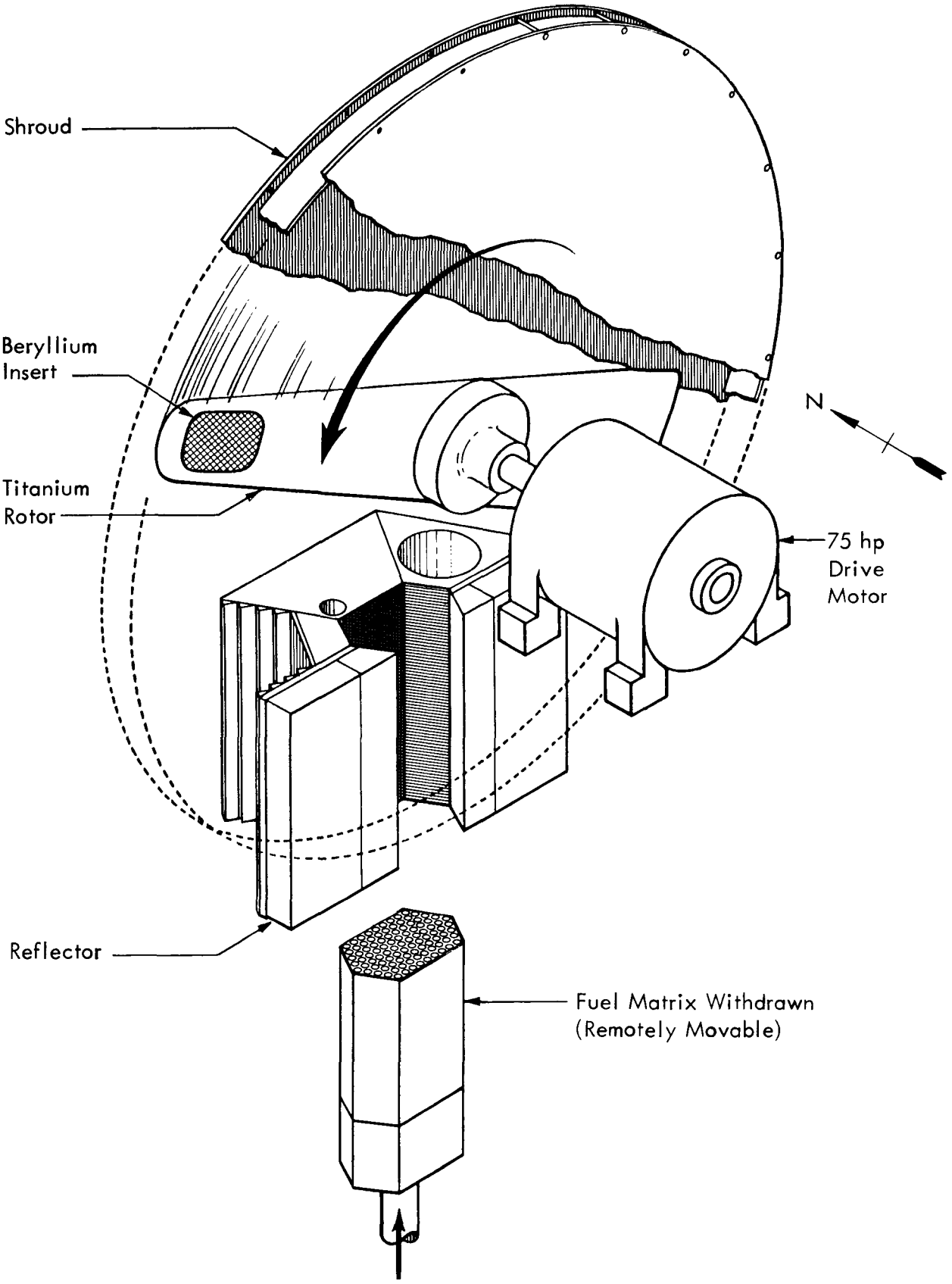

Fig. 5. Pictorial Drawing of the Assembly.

MEASUREMENTS WITH THE ROTOR STATIONARY

After the critical configuration was established, measurements were made to determine the parameters which could be used for theoretical predictions of the results of the repetitively pulsed experiments. The measurements with the rotor stationary included the reactivity of the movable beryllium reflector as a function of the displacement along the path of motion, the fission rate distribution throughout the core from which the peak-to-average power density ratio was obtained, the thermal neutron fluence at the outer surface of the polyethylene scatterer per fission in the core, and the prompt neutron decay constant of the assembly as a function of reactivity. The assembly at delayed criticality contained 87 11/16 fuel rods (core loading pattern No. 8 of Appendix A) with a total uranium mass of 58.6 kg.

Reactivity of the Movable Beryllium Reflector

The reactivity of the movable beryllium reflector as a function of displacement across the unreflected core face was measured with an analog computer which has previously been described.[14] The reactivity as a function of displacement of the beryllium, given in Fig. 6, was fitted over the central 10 cm by least squares techniques to the function $\rho(x) = A + \alpha_x(x-x_0)^2 + c(x-x_0)^4$. The value of α_x thus determined, 3.03 ± 0.03 cents/cm^2, was not as large as those previously measured for the SORA mockup.[11] Since the reactivity in these experiments was 50 cents or more below prompt criticality, the pulse shape in these repetitively pulsed experiments was not as dependent on α_x. The pulse decayed appreciably before the motion of the rotating reflector could produce a significant change in the reactivity of the assembly. The total worth of the beryllium reflector was 4.8 dollars.

---

14. Cesar A. Sastre, Nucl. Sci. Eng. 20, 60 (1964).

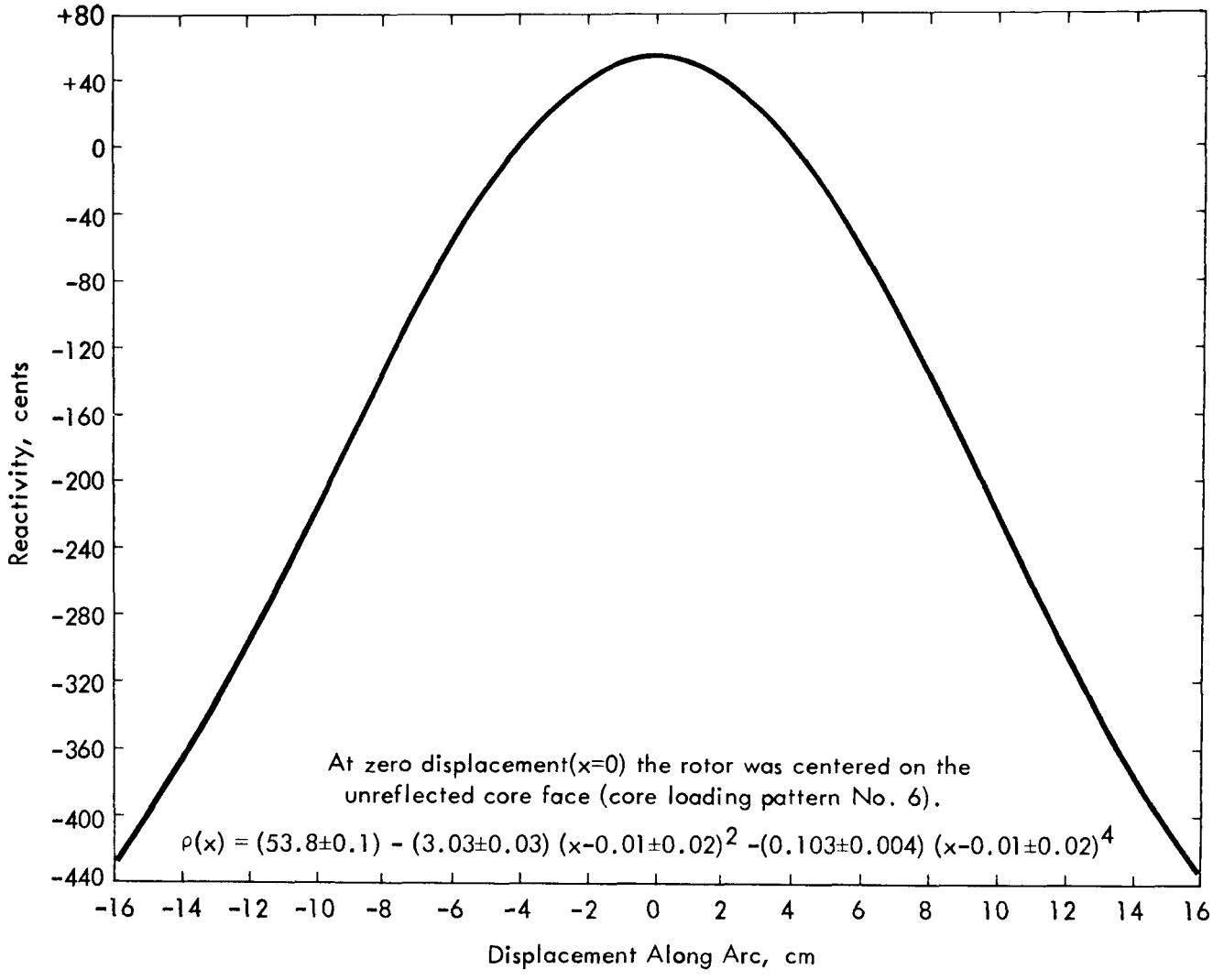

Fig. 6. Reactivity of the Assembly as a Function of the Dispalcement of the Movable Beryllium Reflector Along the Path of Motion.

Fission Rate Distributions

Uranium (93.2 wt % ^{235}U) foils, 0.750 cm in diameter and 0.013 cm in thickness, were activated at various positions in the core to obtain the fission rate distribution throughout the core. The foils were located coaxially with the fuel rods at various vertical positions as shown in Figs. 7 through 9. The peak to average fission density ratio of 1.86 was obtained from these measurements and their interpolation to the unmeasured locations. This ratio was necessary for the determination of the thermal neutron fluence at the outer surface of the scatterer per fission in the core.

Thermal Neutron Fluence at the Scatterer Per Fission

In order to obtain the useful thermal neutron fluence per fission available at the end of the beam tubes for a reactor of this type with this polyethylene scatterer, 1.27-cm-diam, 0.013-cm-thick gold foils were activated on the outer vertical 10.16 x 10.16 cm surface of the scatterer. A pair of bare and a pair of cadmium (0.051-cm-thick) covered foils were located at the ends of a diagonal of a 3.17 cm square centered in this surface of the scatterer. The sides of this square were parallel to the edges of the scatterer. The gamma-ray activity of the foils was observed with a 3.81-cm-diam NaI scintillation counter and converted to thermal neutron fluence[15] at the time of irradiation. The average ratio of the bare foil activity to that of a cadmium covered foil was 2.28 ± 0.12. Simultaneously with the gold foil irradiation, a 667 g sample of 93.2 wt % ^{235}U enriched uranium was irradiated in fuel rod location No. 48. The number of fissions in the sample was determined from the ^{89}Sr content of the uranium sample assuming 0.0465 atoms of ^{89}Sr were produced per fission. The number of fissions in the entire core was obtained from the ratio of the average fission density in the core to the number of fissions in the sample and the mass of the core. The number of thermal neutrons leaking out the outer surface of

15. J. W. Poston, K. W. Crase, and E. M. Robinson, "Thermal Neutron Fluence Measurement in the DOSAR Facility Thermal Pile," ORNL-TM-2009, Oak Ridge National Laboratory (1967).

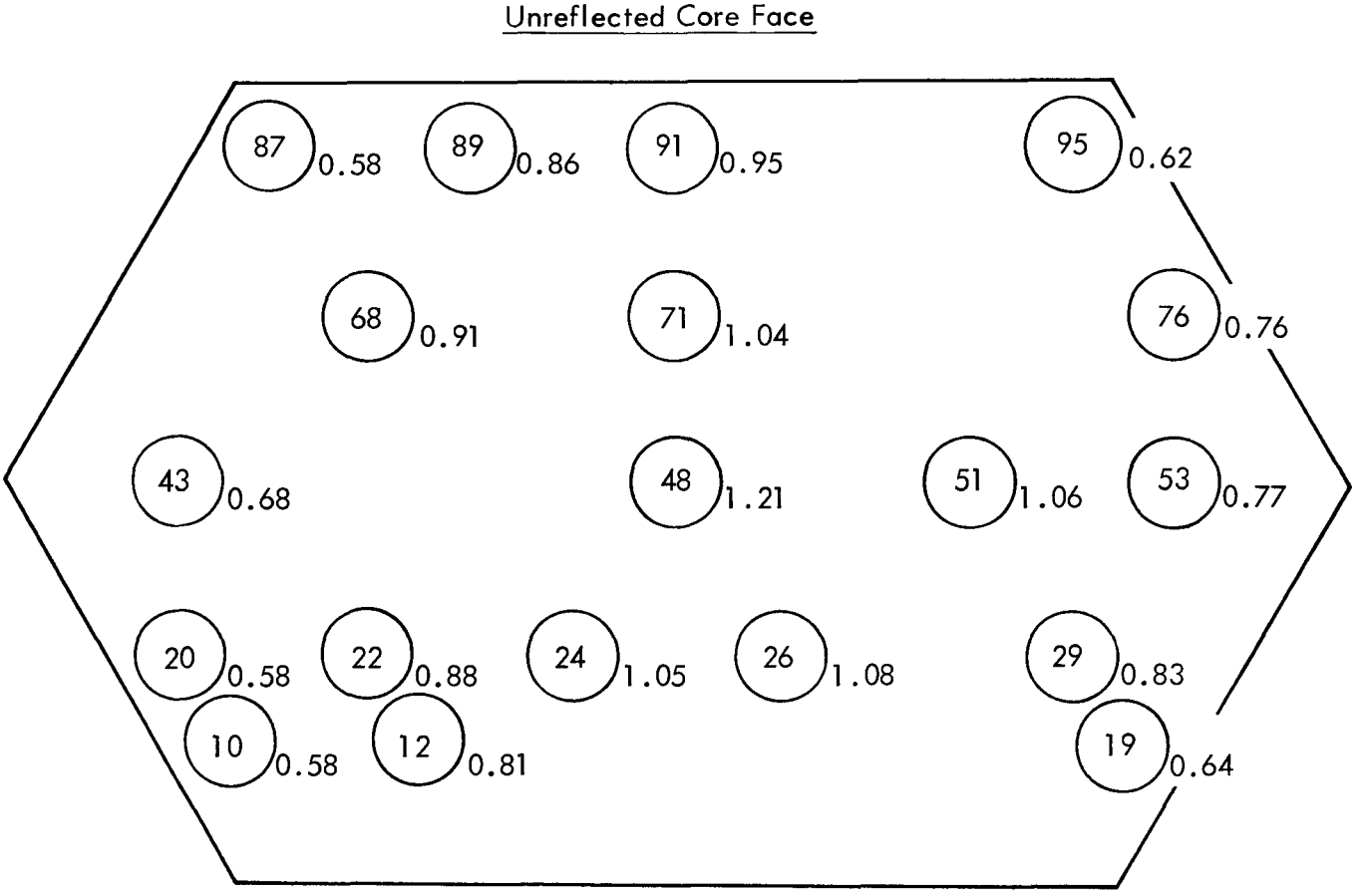

Numbers to the right of circles are relative fission rates at the fuel rod locations given within the circles (core loading pattern No. 5).

Fig. 7. Relative Fission Rate Distribution at the Horizontal Midplane of the Core.

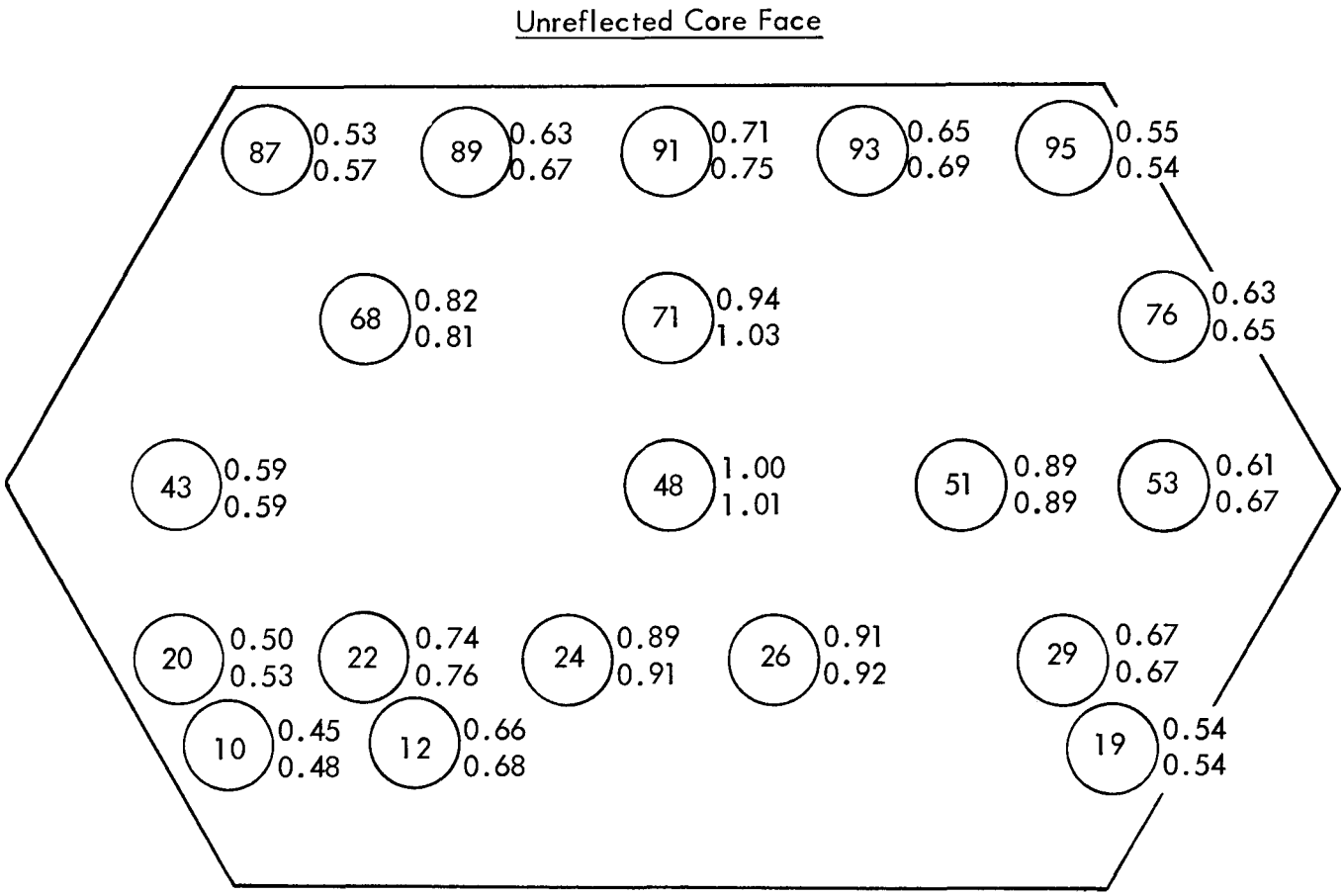

The upper (lower) number to the right of a circle is the relative fission rate 6 cm above (below) the horizontal midplane of the core at the fuel rod location given within the circle (core loading pattern No. 5).

Fig. 8. Relative Fission Rate Distribution in Horizontal Planes 6 cm Above and Below the Midplane of the Core.

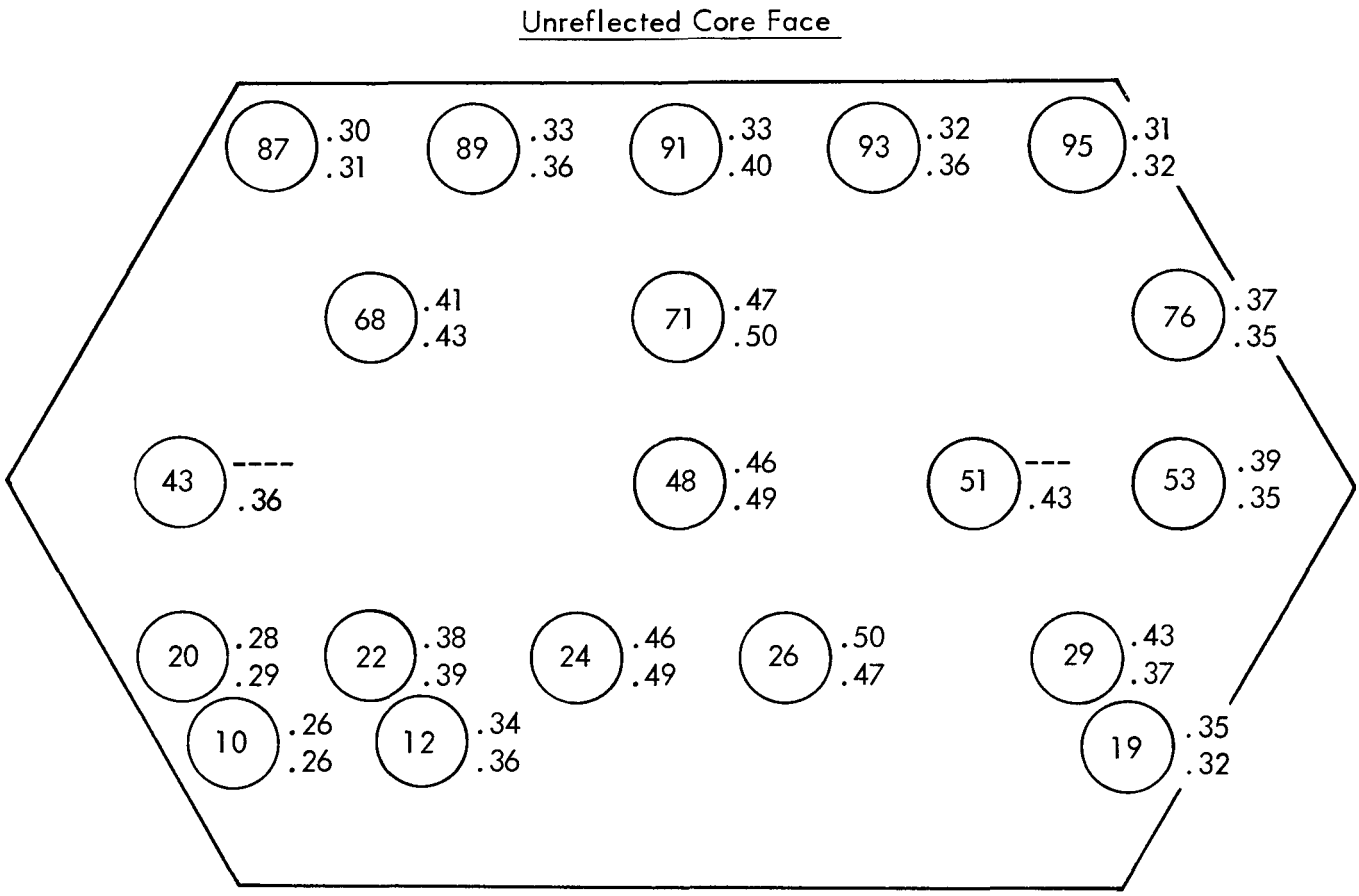

The upper (lower) number to the right of a circle is the relative fission rate at the top (bottom) of the fuel rod in the location given within the circle (core loading pattern No. 5).

Fig. 9. Relative Fission Rate Distribution in Horizontal Planes at the Top and Bottom of the Core.

the polyethylene scatterer at the location of the foils was 3.3×10^{-5} n/cm^2 fission. Two measurements of the thermal fluence at the outer surface of the scatterer per fission agreed to within 2%. The thermal fluence at the foil locations was 15% lower than at the center of the outer surface of the scatterer. The ratio of thermal to epithermal neutrons obtained from measurements with bare and cadmium covered BF_3 counters was 6.3 ± 0.3.

Prompt Neutron Decay

The Rossi-α technique was used to measure the two components of the prompt neutron decay. One plastic scintillator detector (5.1 cm diam, 0.63 cm thick) was located in the top reflector at the core-reflector interface and the other (5.1 cm diam, 1.27 cm thick) was located in the side reflector as shown in Figs. 2 and 3. The time distribution of counts in the second detector was measured with respect to a count in the first. For the measurements with the assembly subcritical, a neutron source was located adjacent to the shroud opposite the center of the unreflected core face.

The prompt neutron decay constants at delayed criticality (see Fig. 10) with the movable beryllium reflector at its maximum reactivity position were 0.36 ± 0.02 μsec^{-1} and 0.12 ± 0.01 μsec^{-1}. These decay constants were larger than those previously reported[11] for the SORA mockup with a movable beryllium reflector because both the beryllium and iron reflector were thinner in the modified assembly.

The prompt neutron decay as a function of fuel loading with the movable beryllium reflector at its maximum reactivity position is given in Fig. 11. For the assemblies with large negative reactivities (≥ 5 dollars), an estimate of the half width of the pulse in a repetitively pulsed experiment can be obtained from these curves. These estimates are accurate as long as the neutron decay is rapid during the time interval required for the rotor motion to change the reactivity of the assembly.

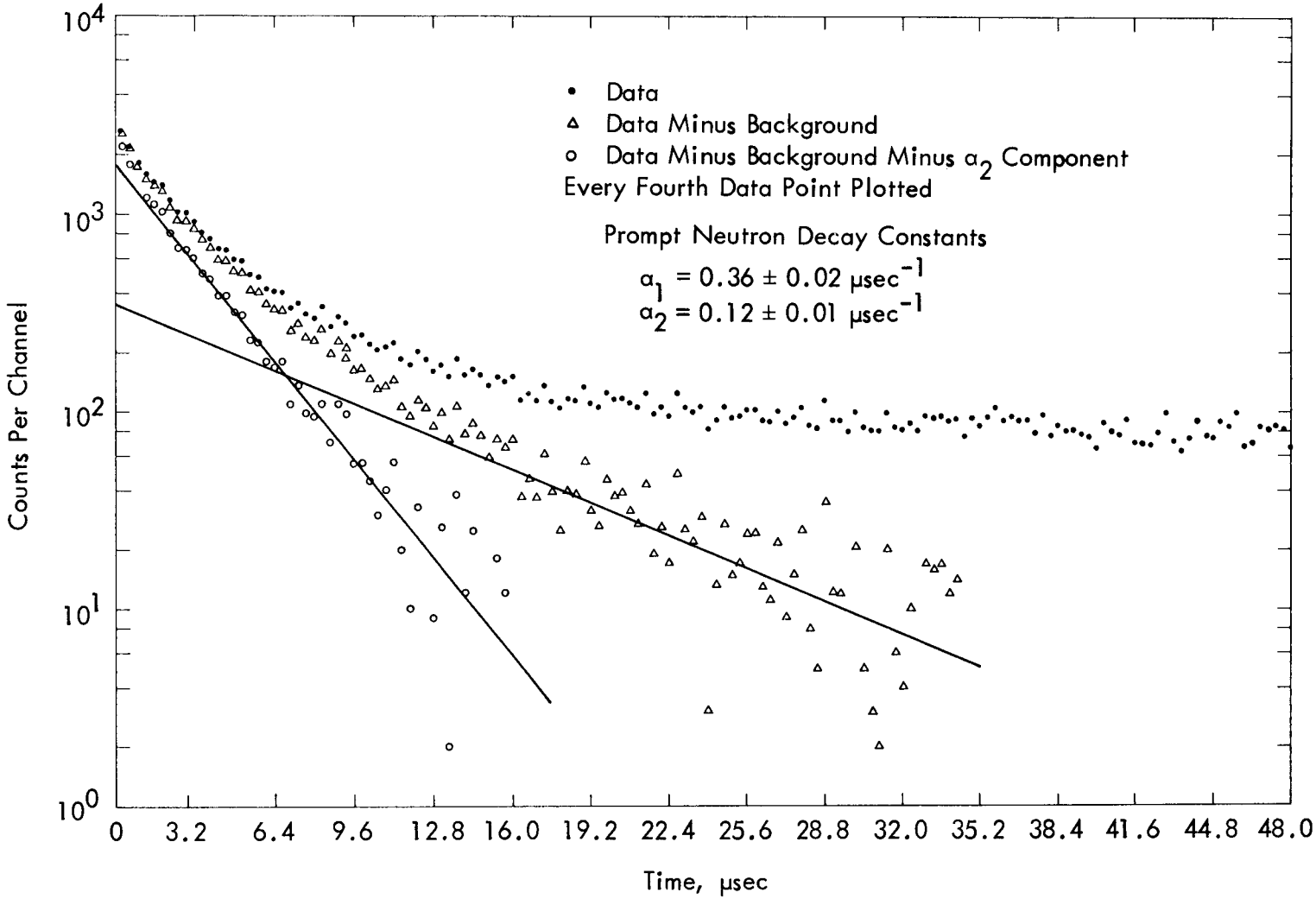

Fig. 10. Prompt Neutron Decay from Rossi-α Measurements at Delayed Criticality with the Movable Beryllium Reflector at the Position of Maximum Reactivity.

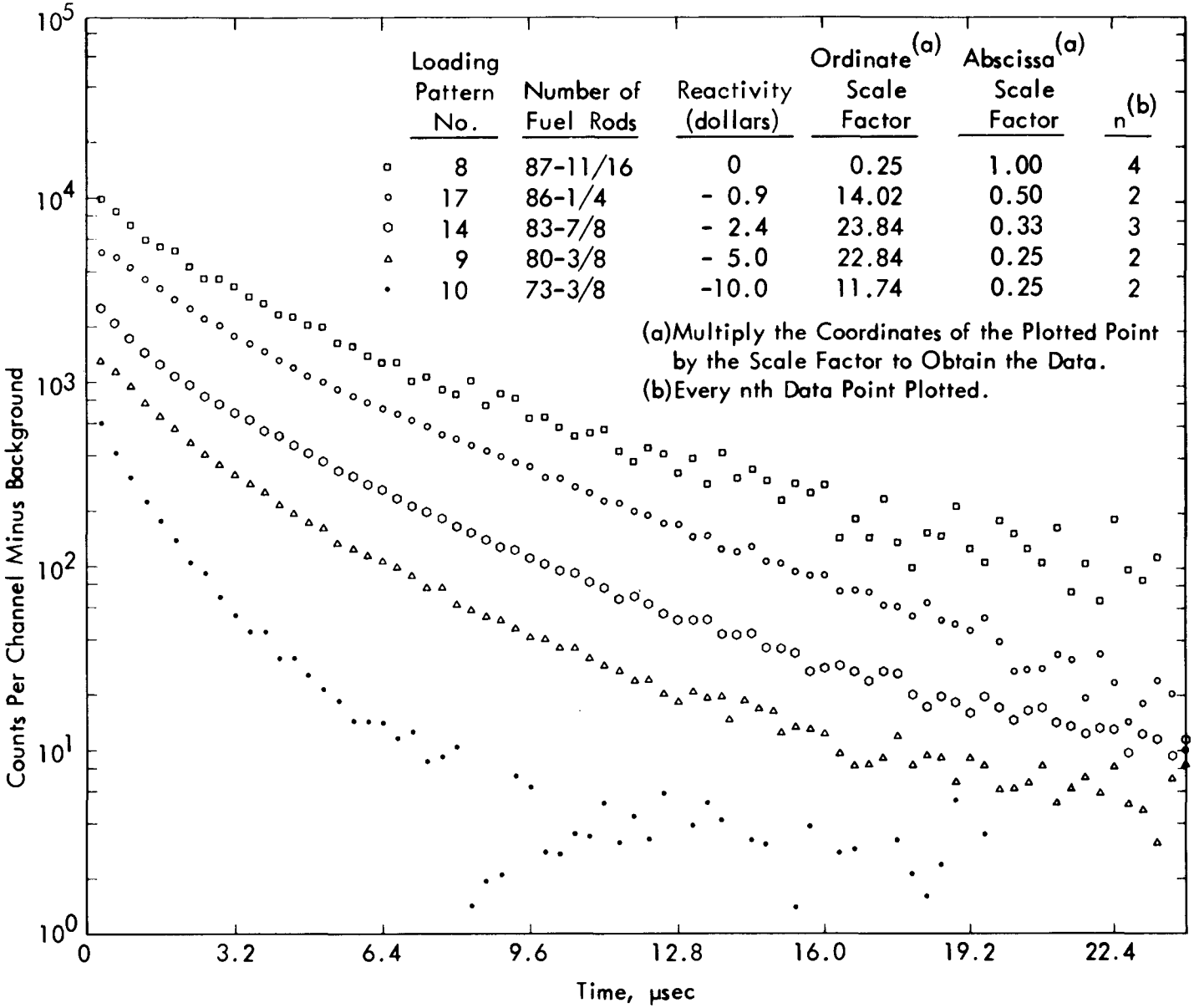

Fig. 11. Prompt Neutron Decay from Rossi-α Measurements with the Movable Beryllium Reflector at the Position of Maximum Reactivity for Various Fuel Loadings.

The prompt neutron decay for the assembly of 86 11/16 fuel rods, with the movable reflector displaced 4 cm to the west (see Fig. 2 for direction of west) in order to maintain the system at delayed criticality, is shown in Fig. 12. The neutron decay with the movable beryllium reflector displaced 9.7 cm to the west is also shown in Fig. 12. The data presented in this figure illustrates the dependence of the prompt neutron decay on the position of the movable beryllium reflector.

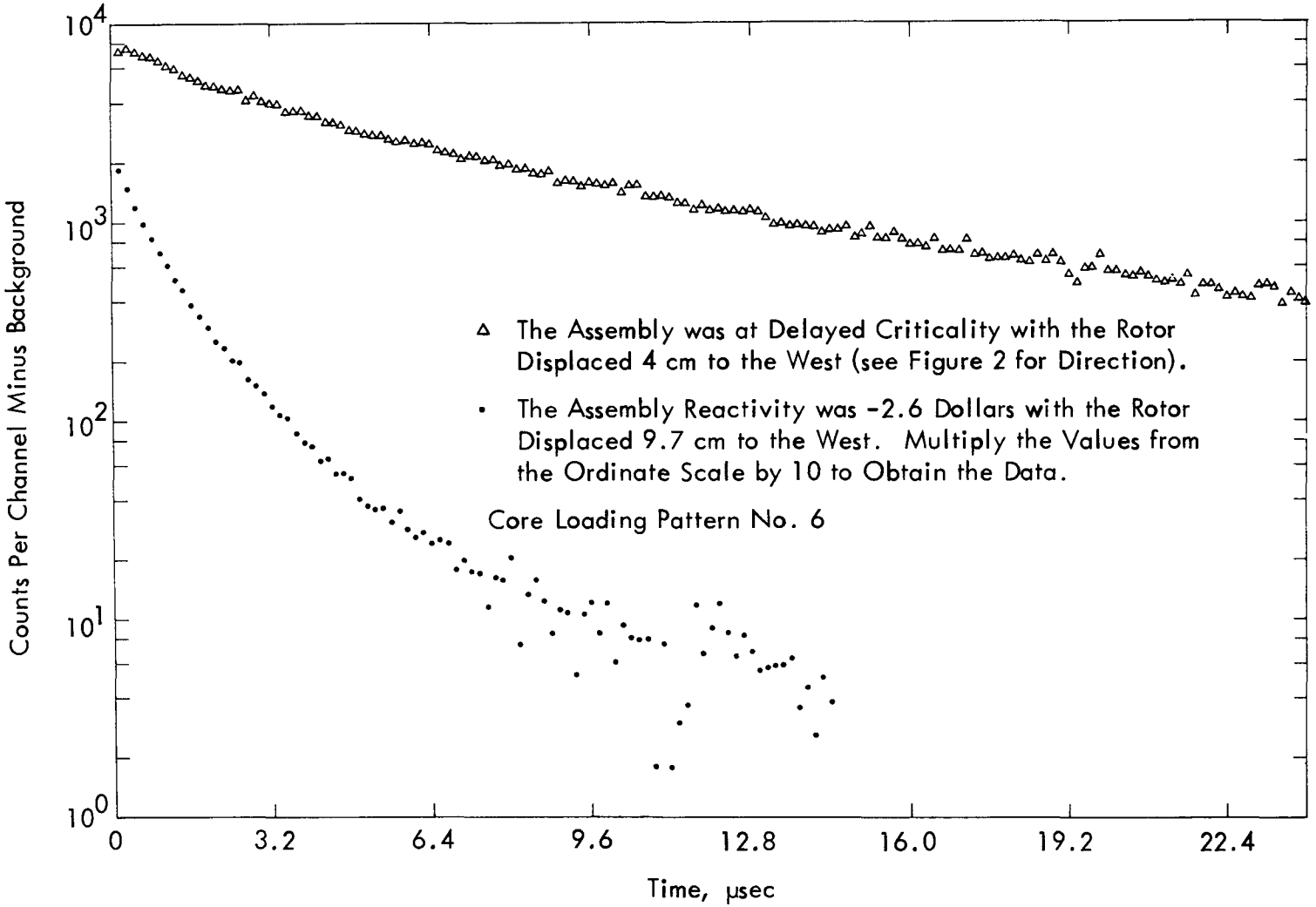

Fig. 12. Prompt Neutron Decay from Rossi-α Measurements with the Movable Beryllium Reflector Displaced from its Maximum Reactivity Position.

REPETITIVELY PULSED EXPERIMENTS

After the measurements with the rotor stationary, a series of experiments with the rotating reflector moving past the unreflected core surface ~60 times/sec at a speed of 264 meters/sec was performed. The time distributions of the neutron density in the core, in the reflector, and at the outer surface of the polyethylene scatterer were measured after the injection of an ~1-μsec-long pulse of 14.1 MeV neutrons by a Cockcroft-Walton accelerator each time the rotating reflector attained its maximum reactivity position. The effect of varying the reactivity on the time distribution of neutrons was determined for reactivities between 95 cents below and 50 cents above delayed criticality. The corresponding variation in the prompt neutron multiplication was between 73 and 285 if the effective delayed neutron fraction was 0.007. These measurements determined the pulse characteristics of this assembly when used as a repetitively pulsed booster. One group neutron kinetics was used to interpret some of the measurements.

Method of Assembly

The system was assembled to delayed criticality and the reactivity determined with the movable beryllium reflector at its maximum reactivity position as described previously. This maximum reactivity position of the movable beryllium reflector was verified prior to each repetitively pulsed operation. After this verification, the system was shut down by lowering the vertical lift which supported the core and bottom reflector. The reactivity was manually adjusted to the desired value by changing the fuel loading. The rotation of the movable reflector was then initiated. After a short time required for the rotating system to come to mechanical equilibrium, the core and bottom reflector were inserted into the top and side reflector in the presence of a neutron source. After core insertion, the Pu-Be neutron source was replaced by the pulsed neutron source. The pulse characteristics of the assembly were measured after the mechanical and thermal effects of the rotor had equilibrated. Nuclear shutdown by lowering the core preceded shutdown of the rotating system.

Instrumentation

The instrumentation consisted of a means of triggering the accelerator pulse and the time analysis equipment whenever the rotating reflector passed through the position of maximum reactivity, neutron detectors which measured the time distribution of neutrons at various locations in the assembly, time analysis equipment which recorded these distributions, and of the devices which indicated the condition of the rotating assembly. The last are described in Appendix B.

An inductive type radio frequency proximity gauge developed by Ellis[16] provided a signal which, after delay, triggered the time analysis equipment and the accelerator pulse. This gauge was mounted on the shroud ~1/4 of a revolution in advance of the maximum reactivity position of the rotor. The delay was adjusted so that the pulse of neutrons was produced by the accelerator at the time the rotating reflector was at the position for which the reactivity of the assembly was maximum. The time analysis equipment was triggered before the accelerator produced the neutron pulse so that all of the time distribution of neutrons could be recorded.

The detectors providing the time distribution of neutrons at various locations in the assembly (see Figs. 2 and 3) were BF_3 proportional counters or proton recoil scintillators. A pair of 2.54-cm-long, 0.79-cm-diam proportional counters was located adjacent to the outer surface of the polyethylene scatterer with the long dimension vertical. The counters were centered vertically on this surface and were located 1.5 cm from its center. One was covered with 0.063-cm-thick cadmium. These counters were enclosed by the cadmium that covered the surfaces of the polyethylene. Thus, the counter without cadmium did not detect thermal neutrons scattered back from the surrounding walls of the room which were more than 3.1 meters away. A third BF_3 counter of the same size was situated at the horizontal midplane of the core in fuel rod location No. 58. A 2.54-cm-diam, 20.64-cm-long BF_3 proportional counter was

16. J. F. Ellis, Trans. Amer. Nucl. Soc. 11, 342 (1968).

located in the side reflector. A plastic scintillator was located at the core-top-reflector interface in the 5.72-cm-diam hole in the top reflector. A second plastic scintillator was positioned immediately below the target assembly of the accelerator in the side reflector. The discrimination level of this latter scintillation counter system was set to reject neutrons with energies below 14.1 MeV. Thus, the time distribution of the source neutrons injected into the assembly by the accelerator could be measured with the scintillator near the accelerator target.

The time analysis equipment consisted of a time interval counter and a PDP-4 digital computer which processed the binary information from the time interval counter. The time base was established by a 10 Mc crystal oscillator. The time interval counter measured the times between the delayed reference signal from the proximity gauge and the count signals from the detectors. The PDP-4 stored the counts according to the length of these time intervals. The time analysis equipment was triggered once per revolution of the rotor and each time distribution that the analyzer recorded was an accumulation over many revolutions. The time distribution of events in up to four detectors could be processed and stored independently by this equipment. The delay between an event in a particular detector and the arrival of its signal at the time analysis equipment was adjusted by delay cable. This delay for each detector was different so that the time analysis equipment was not required to process data at high rates from the four detectors simultaneously. For example, the delay for the cadmium covered detector at the outer surface of the scatterer was such that the peak of this time distribution occurred after the time distribution of neutrons in the core had decreased a factor of 10^3 from its maximum value. As a result, the counting losses by the time analysis equipment were less than a few percent and no corrections were made.

In order to be able to measure the pulse shape in detail and the time distribution over the entire 16.6 msec between pulses, the 1024 data storage channels of the time analysis equipment were of unequal channel width. The channels were divided into groups of 400, 100, 50,

50, and 243. The widths of the second, third, fourth, and fifth groups were a factor of 2, 4, 8, and 256, respectively, larger than that of the first group of channels. After the initial measurements showed that the time distribution of neutrons was constant prior to the production of the pulse by the accelerator, the analysis time was reduced from 16.6 to 10 msec.

Pulse Characteristics

The widths of the neutron pulses from the accelerator varied from experiment to experiment as shown in Fig. 13. The accelerator pulse widths at half maximum were 0.95, 1.00, 0.70, and 0.80 μsec, respectively, for the experiments with the assembly with reactivities of -95, -5, +26, and +50 cents. These reactivities were obtained from those measured in the experiments with the rotor stationary by subtracting the reactivity change due to the increase in the temperature of the core and to the small lateral displacement of the rotor from the core. The total change in reactivity from these effects was ~5 cents.

The time distributions of neutrons in the core, measured with a BF_3 proportional counter in fuel rod locations No. 58, are shown in Fig. 14 for the assembly with reactivities of -95, -5, and +50 cents. The characteristics of these distributions are listed in Table 1. A fit of the function, $n(t) = A + B \exp(-\alpha_1 t) + C \exp(-\alpha_2 t)$, to the time distribution of neutrons after the accelerator pulse for the assembly with a maximum reactivity of 50 cents gave prompt neutron decay constants of 0.129 ± 0.001 and 0.0016 ± 0.0001 μsec^{-1}. However, the distribution of the signs of the residuals was not random; that is, the residuals were negative for channels 42 to 108 and positive for channels 189 to 521. This indicated that because of the motion of the rotor, the function assumed did not adequately represent the data over the complete time interval of the measurements although the results of the Rossi-α measurement with the rotor stationary had been successfully fitted to this function (see Fig. 10).

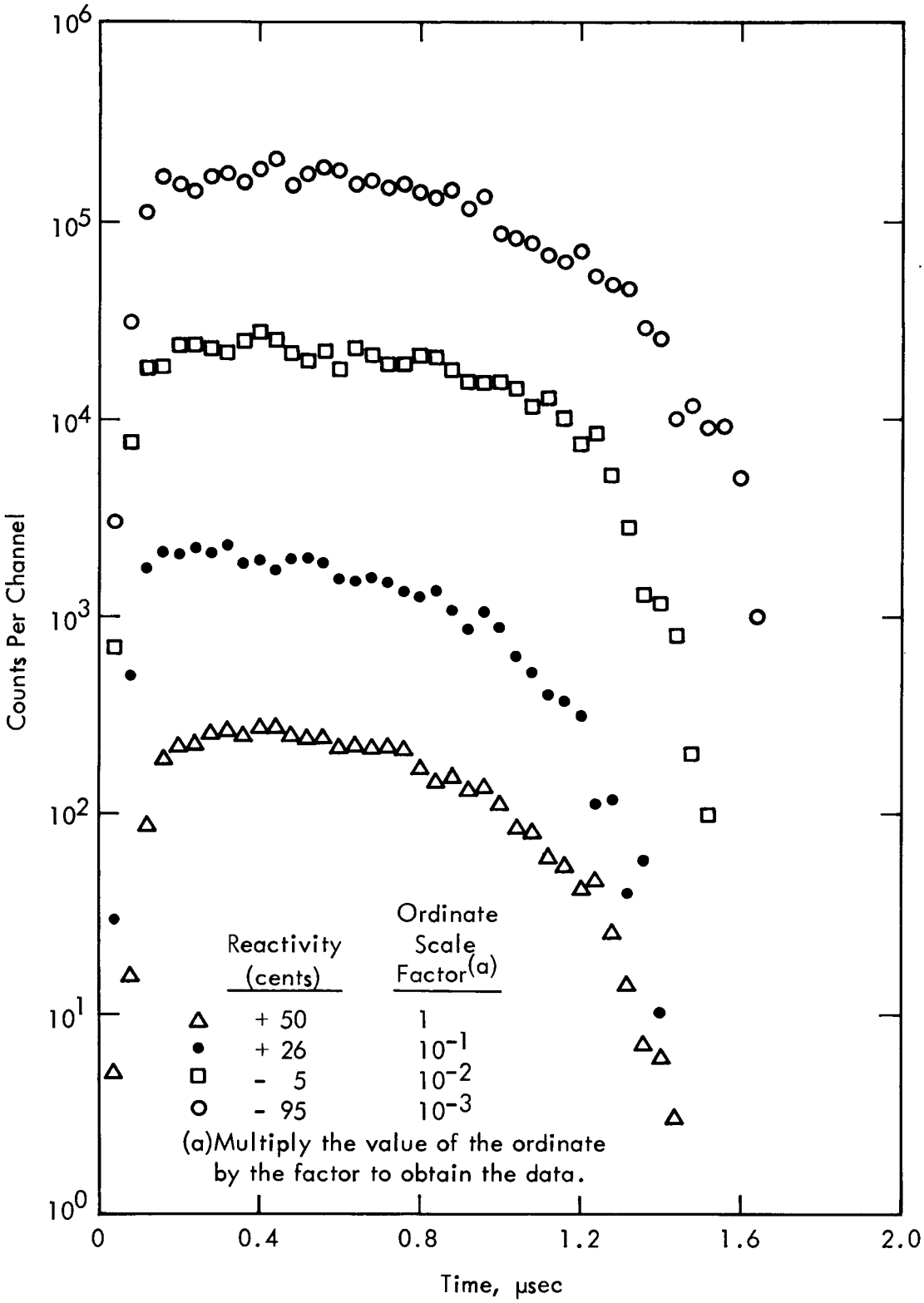

Fig. 13. The Time Distribution of Neutrons from the Cockcroft-Walton Accelerator in the Repetitively Pulsed Experiments.

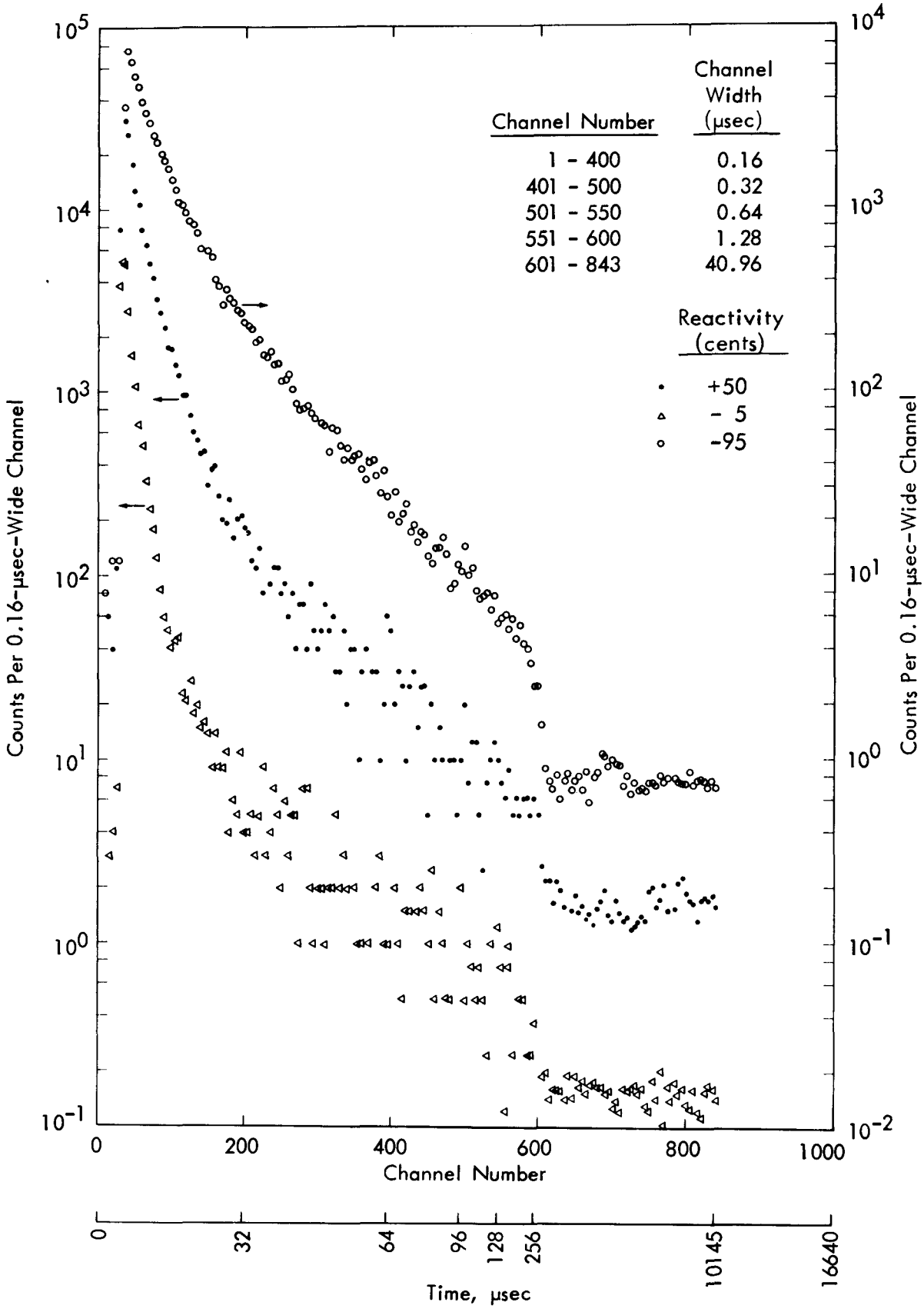

Fig. 14. The Time Distribution of the Neutrons in the Core in the Repetitively Pulsed Experiments for the Assembly with Maximum Reactivities of +50, -5, and -95 cents.

Table 1. The pulse Characteristics of the Assembly for Various Values of the Maximum Reactivity.

Core Loading Pattern Number[a]	Maximum Reactivity (cents)	Maximum Prompt Neutron Multiplication[b]	Pulse Width at Half Maximum[c] (μsec)			Ratio of the Neutron Density the Peak of the Pulse to the Neutron Density Between Pulses		
			BF_3 Detector in Core	Cd Covered BF_3 Detector at the Scatterer	BF_3 Detector at the Scatterer	BF_3 Detector in Core	Cd Covered BF_3 Detector at the Scatterer	BF_3 Detector at the Scatterer
12	50	285	3.9(15.0)	7.4(20.9)	28(93.7)	12,400	7,400	1,590
15	26	190	3.1(10.9)	5.0(17.9)	--	18,100	9,000	--
8	- 5	135	2.7(8.6)	5.2(12.9)	21(82.0)	22,400	12,300	2,500
17	-95	75	2.3(5.5)	4.0(8.9)	--	39,300	20,200	3,200

a. See Appendix A for core loading.
b. Calculated with $\beta_{eff} = 0.007$.
c. The effective normal mode decay constants obtained from these pulse widths at half maximum were 0.20, 0.25, 0.32, and 0.39 μsec^{-1} for the assembly with maximum reactivities of +50, +26, -5, and -95 cents, respectively. The numbers in parentheses are the widths of the pulse at 10% of the maximum amplitude of the pulse.

The expression for the power pulse half width given by Larrimore,[17]

$$\theta = \alpha^{-1} \ln [1 + \exp(\alpha t_a)], \qquad (1)$$

where α is the effective normal mode decay constant and t_a is the duration of the neutron pulse from the accelerator, was used to obtain an estimate of the effective normal mode decay constant. The decay constants obtained using Eq. (1), which are given in Footnote c of Table 1, varied from 3.9 to 2.0 μsec^{-1}. The effective one-group normal mode decay constant can be considered a weighted average of the decay constants of the fast (α_1) and slow (α_2) components of the prompt neutron decay from the Rossi-α measurements at delayed criticality with the rotor stationary (i.e., $\alpha = w_1\alpha_1 + w_2\alpha_2$ where $w_1 + w_2 = 1$). The values of w_1 obtained from the values of α inferred from the experiments where maximum reactivities were +50, +26, and -5 cents are 0.35, 0.55, and 0.85, respectively.

The time distribution of epithermal neutrons (those with energies above the 0.063-cm-thick cadmium cutoff energy) at the outer surface of the polyethylene scatterer are shown in Fig. 15 for the assembly with maximum reactivities of -95, -5, and +50 cents. The time distribution of the neutrons of all energies at the outer surface of the polyethylene scatterer is shown in Fig. 16 for the assembly with maximum reactivities of +50 and -5 cents. For the assembly with a maximum reactivity of 50 cents, the neutron pulse widths at half maximum in the core, at the outer surface of the scatterer for the neutrons of all energies, and at the outer surface of the scatterer for the epithermal neutrons were 3.9, 28, and 7.4 μsec, respectively. Thermalization by the scatterer produces a broadening of the pulse from 3.9 to 28 μsec. The decay of all neutrons and of the epithermal neutrons obtained from pulsed neutron measurements with the scatterer alone are given in Appendix C.

The time distributions of the neutrons for 24 μsec after the accelerator pulse in the core and at the outer surface of the polyethylene scatterer are shown in Figs. 17, 18, and 19 for the assembly with maximum reactivities of +50, -5, and -95 cents. Since in these experiments

---

17. J. A. Larrimore, Nucl. Sci. Eng. 29, 87 (1967).

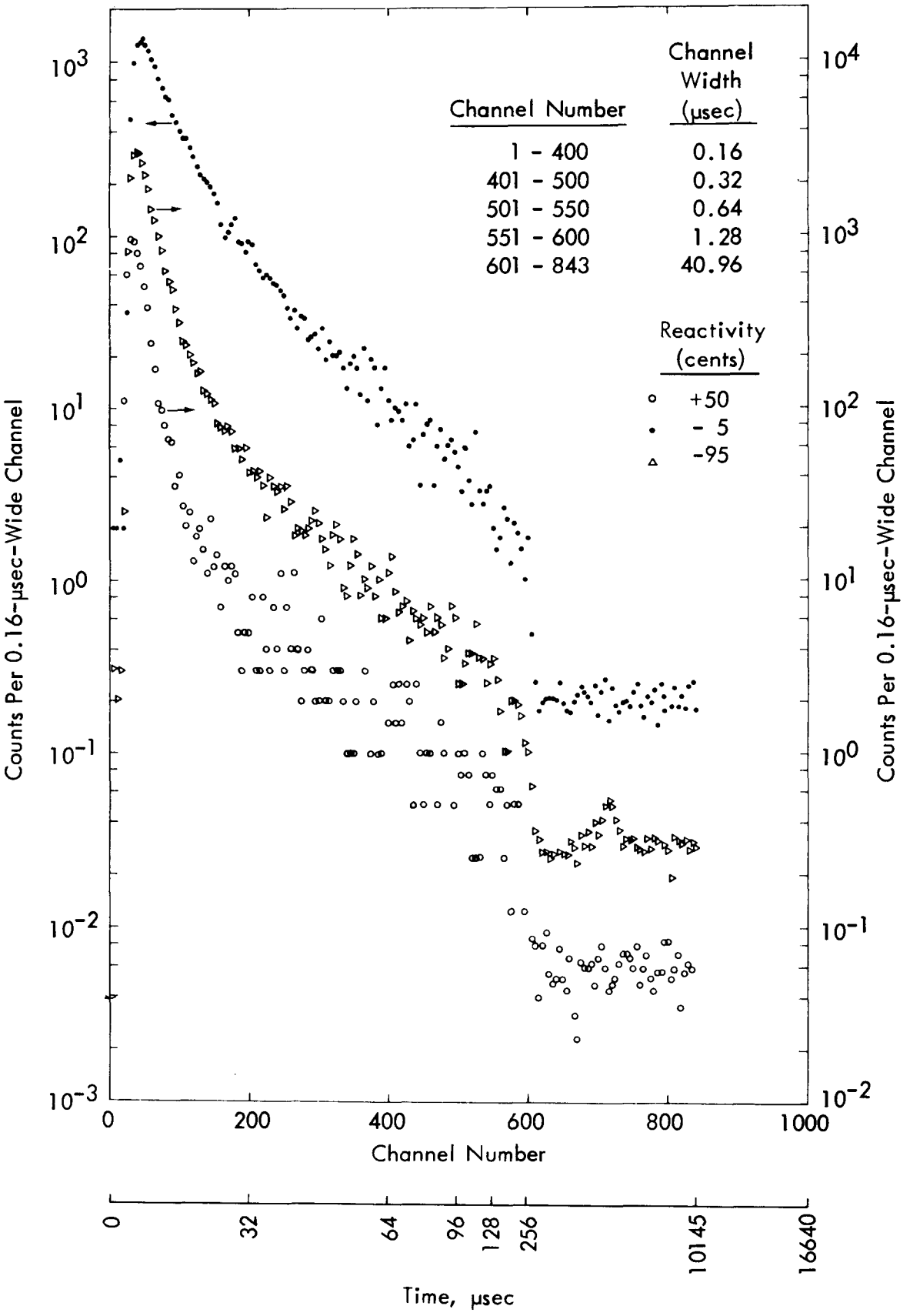

Fig. 15. The Time Distribution of Epithermal Neutrons at the Outer Surface of the Scatterer in the Repetitively Pulsed Experiments for the Assembly with Maximum Reactivities of +50, -5, and -95 cents.

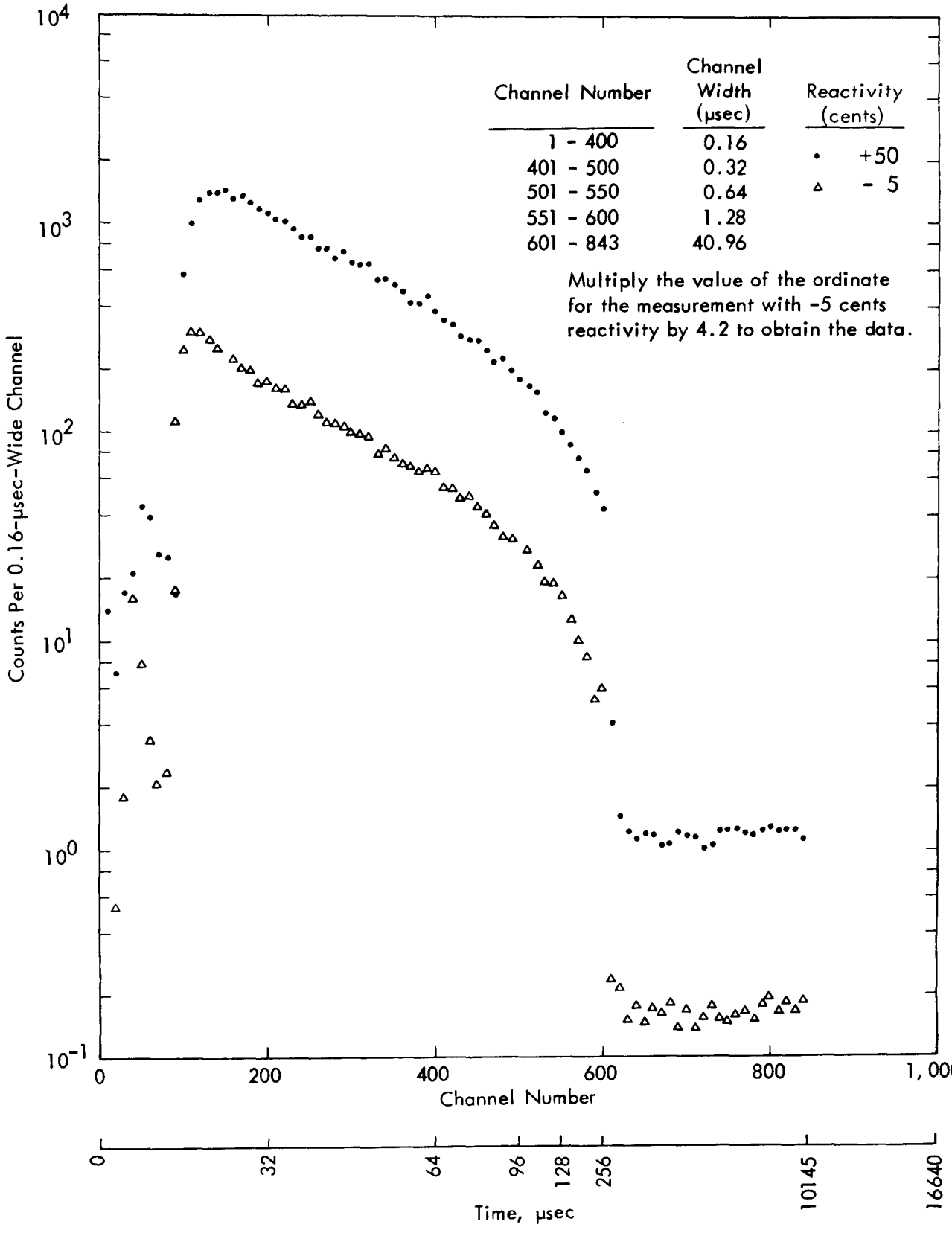

Fig. 16. The Time Distribution of Neutrons of all Energies at the Outer Surface of the Scatterer in the Repetitively Pulsed Experiments for Assemblies with Maximum Reactivities of +50 and -5 cents.

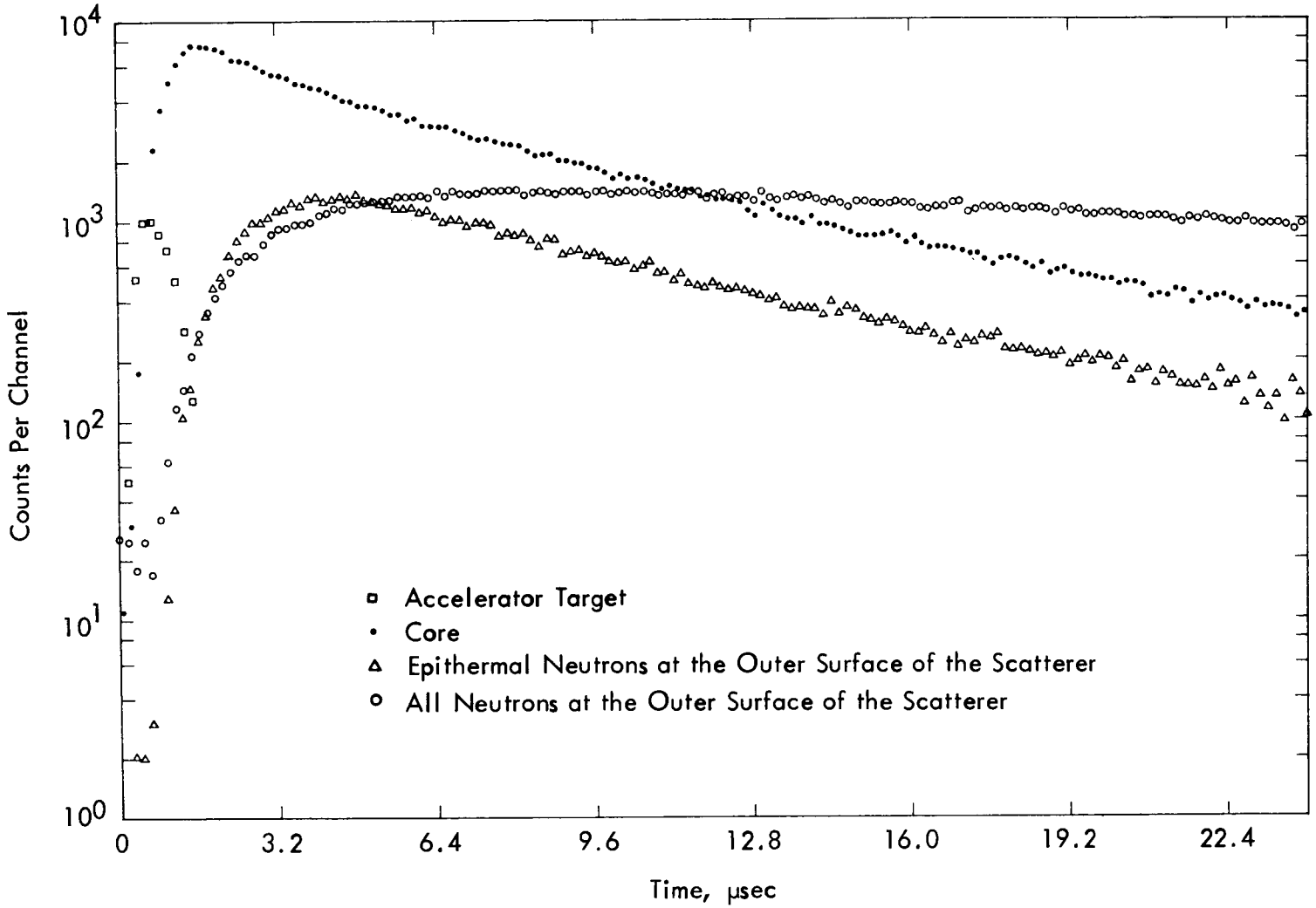

Fig. 17. The Time Distribution of the Neutrons for 24 μsec after the Accelerator Pulse for the Assembly with a Maximum Reactivity of +50 cents.

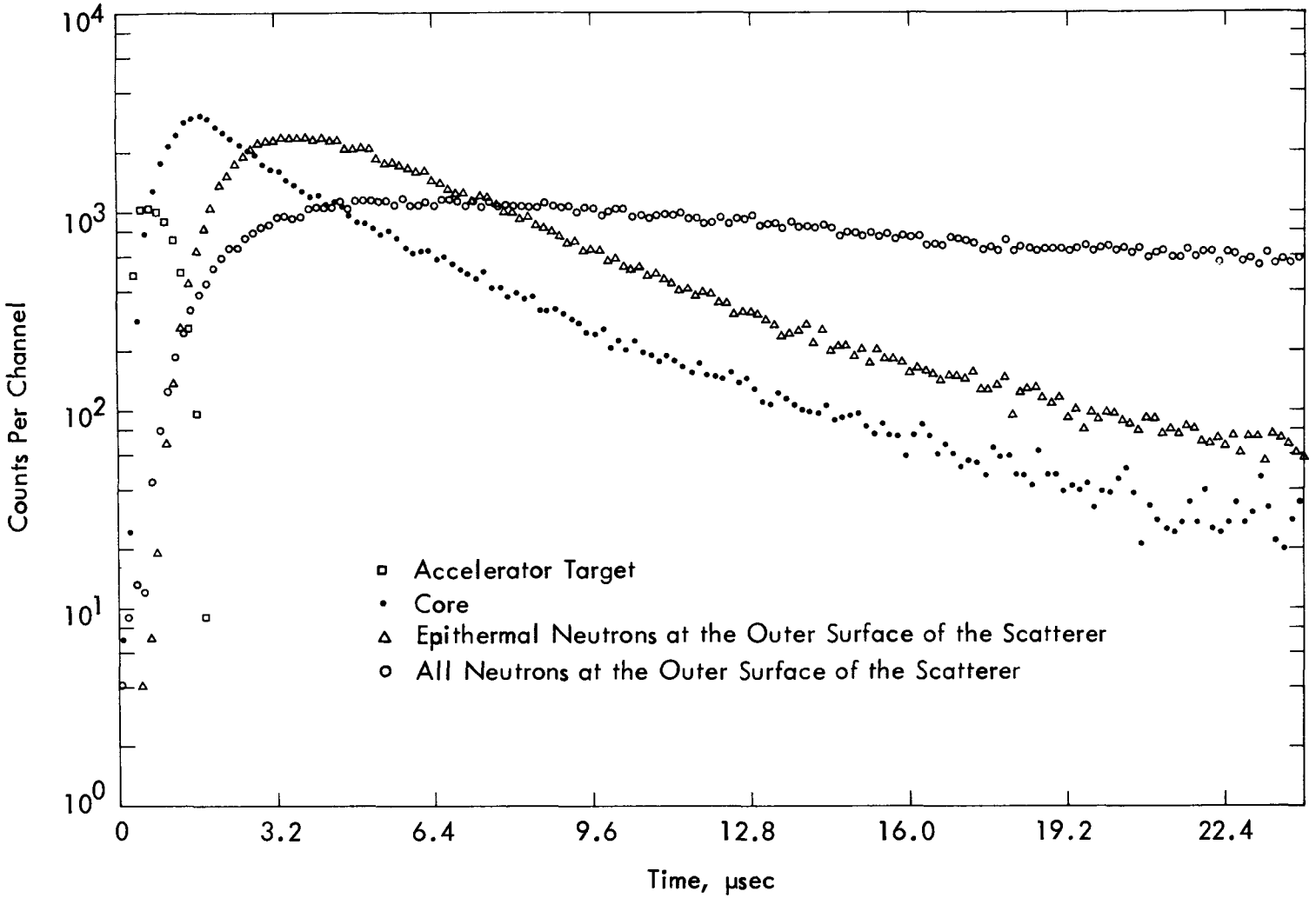

Fig. 18. The Time Distribution of the Neutrons for 24 μsec after the Accelerator Pulse for the Assembly with a Maximum Reactivity of -5 cents.

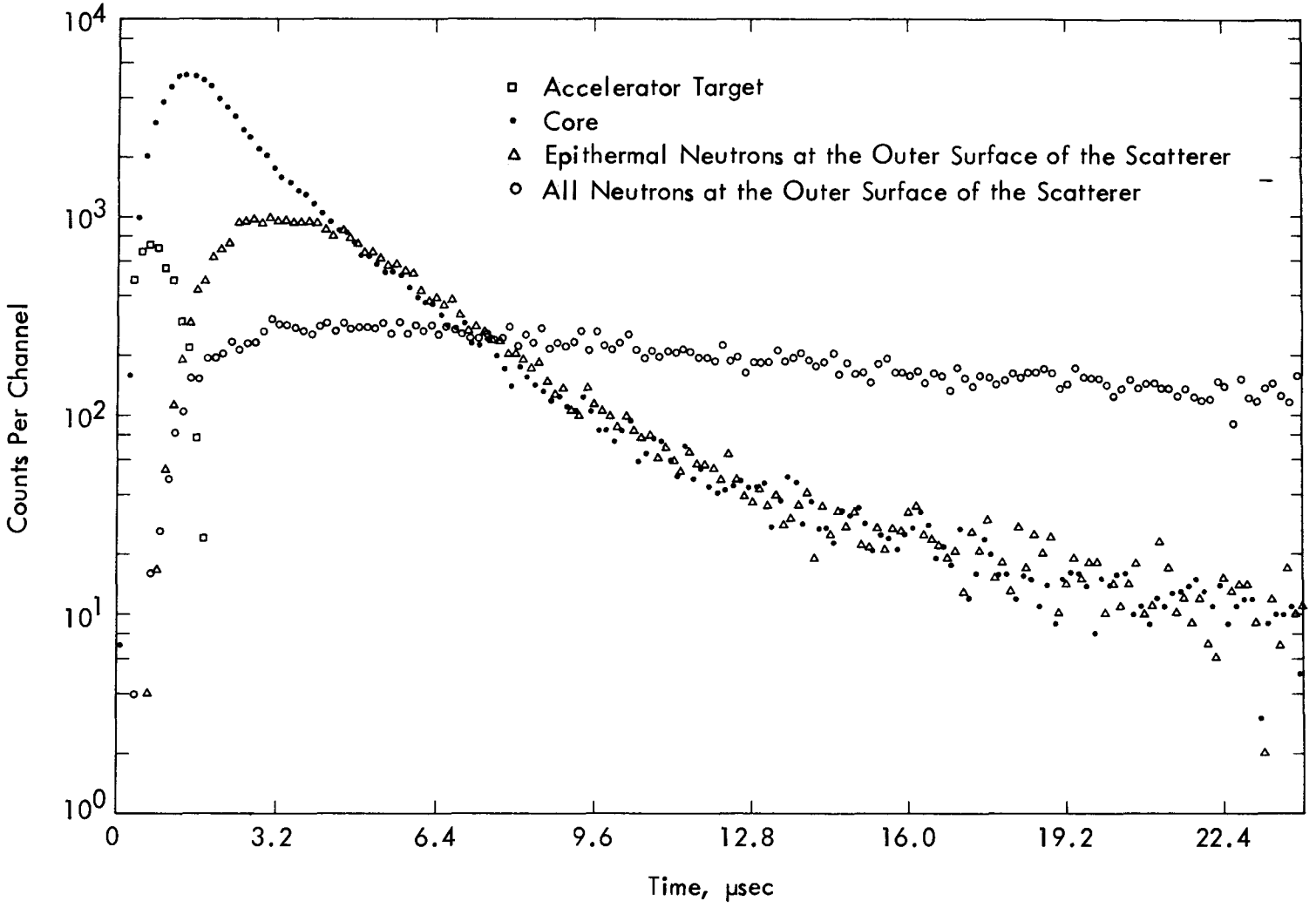

Fig. 19. The Time Distribution of the Neutrons for 24 μsec after the Accelerator Pulse for the Assembly with a Maximum Reactivity of -95 cents.

only the shapes of the pulses were of primary interest, these data have not been corrected for the difference in detector efficiency at the various locations. The peak of the time distribution of the epithermal neutrons at the outer surface of the scatterer for the assembly with a reactivity of +50 cents was attained about 2.7 μsec after that for the neutron pulse in the core. The peak of the time distribution of neutrons of all energies at the outer surface of the scatterer occurred about 4.8 μsec later than that for the epithermal neutrons. These delays result from the neutron slowing-down-time in the scatterer. Corresponding results for the assembly with a reactivity of -5 cents were 2.4 and 3.2 μsec while those for the assembly with a reactivity of -95 cents were 2.1 and 2.4 μsec. The epithermal neutrons decayed at the same rate as the neutrons in the core. Compared to the higher energy neutrons in the core or at the scatterer, the time distribution of the neutrons of all energies at the outer surface of the scatterer was relatively constant after achieving its maximum.

The expression for the fraction of neutrons in the pulse is[17]

$$E_p = 1 - [\rho + A\beta]^{-1} \qquad (2)$$

where ρ is the reactivity of the rotating reflector, A is the prompt neutron multiplication, and β is the delayed neutron fraction. Using a value of the reactivity of the rotating reflector of 4.8 dollars, the prompt neutron multiplications given in Table 1, and a delayed neutron fraction of 0.007, the calculated fraction of all the neutrons that are in the pulse varied from 0.81 to 0.85 where the maximum reactivity varied from -95 to +50 cents. The fraction of all neutrons that are in the pulse, obtained from the measurements with the BF_3 counter in the core given in Fig. 14, were 0.81, 0.80, and 0.80 for the assembly with maximum reactivities of -95, -5, and +50, respectively. These results were in good agreement with those from Eq. (2). The measurements showed that the fraction of all neutrons that are in the pulse was independent of position. For example, the values of this fraction for the assembly with a maximum reactivity of +50 cents for the distribution

of all neutrons in the core, in the reflector, and at the outer surface of the scatterer were 0.80, 0.78, and 0.77, respectively. The value for the epithermal neutrons at the outer surface of the scatterer was 0.80. The fraction of neutrons in the pulse at all detector locations for all reactivities measured was between 0.78 and 0.85.

As shown in Fig. 20, the ratios of the peak neutron density to the minimum between pulses both in the core and at the scatterer are linear functions of reactivity. There were three contributions to the background between pulses: delayed neutrons in the assembly, counts from the counter-detection-system electronics, and neutrons from the accelerator. The last was due to extraneous deuterons which were emitted from the ion source of the accelerator between pulses and produced neutrons at the target. The ratios of the neutron density in the peak of the pulse to the neutron density between pulses, given in Table 1 and in Fig. 20, have been corrected for the accelerator and counter background. For the assembly with a maximum reactivity of +50 cents, these ratios for the neutrons in the core, for the epithermal neutrons at the outer surface of the scatterer, and for neutrons of all energies at the outer surface of the scatterer were 12400, 7400, and 1590, respectively.

The expression for the peak to average power in a pulse is[17]

$$E_p[1 - \exp(-\alpha t_a)]/D \qquad (3)$$

where D is the product of the duration of the accelerator pulse, t_a, and the number of accelerator pulses per second, and the other quantities have previously been defined. The calculated values of this ratio for the assembly with maximum reactivities of -95, -5, +26, and +50 cents were 4400, 3650, 3440, and 2460, respectively. The corresponding experimental values from the time distributions of neutrons in the core were 5200, 3800, 3300, and 2000. The calculated ratios are lower than the experimental at low reactivity and higher than the experimental at high reactivity.

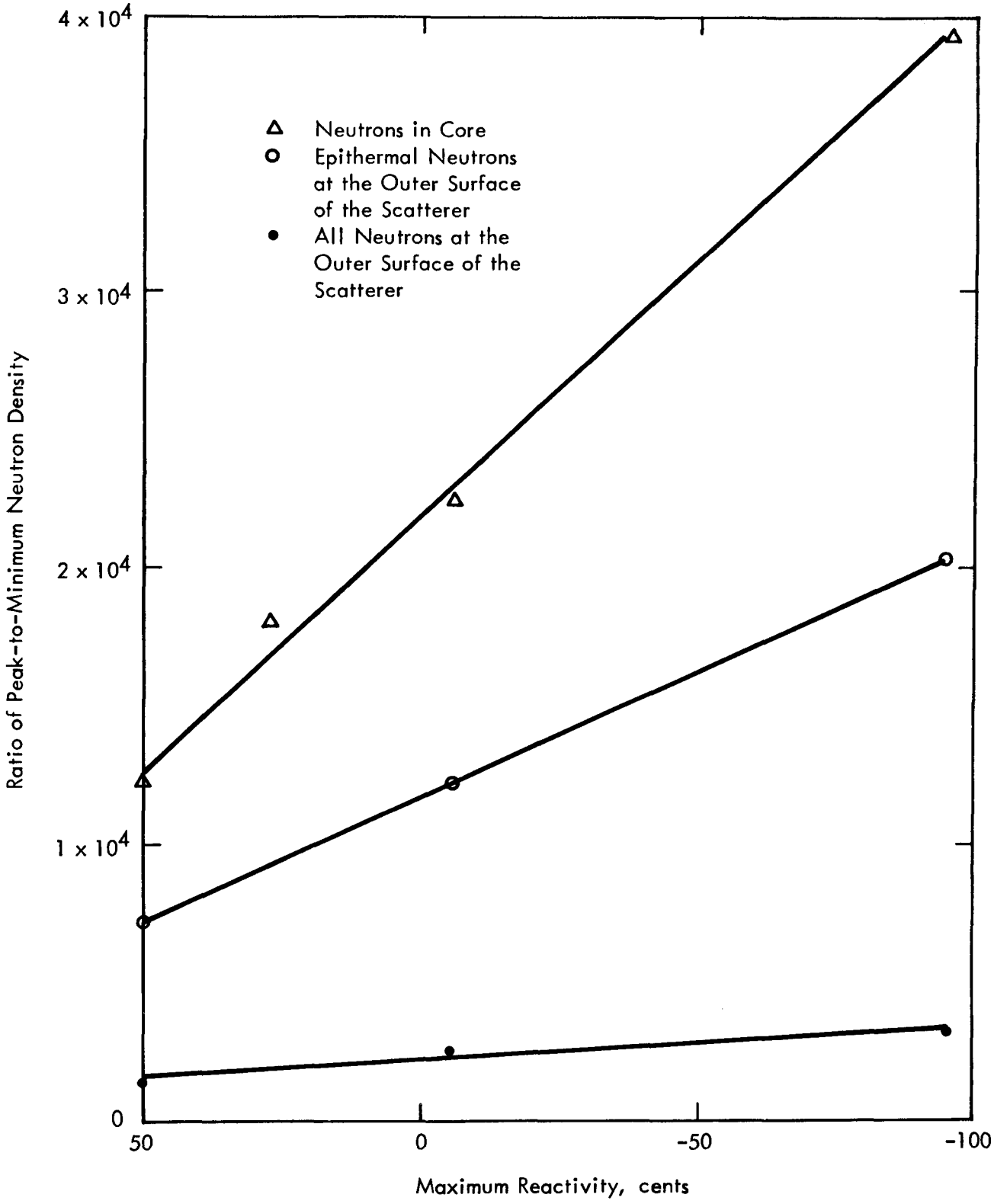

Fig. 20. Ratio of the Neutron Density in the Peak of the Pulse to the Minimum Between Pulses in the Core and at the Outer Surface of the Scatterer as a Function of the Maximum Reactivity.

CONCLUSIONS

This assembly with a maximum prompt neutron multiplication of 285 (50 cents above delayed criticality) can be used with an accelerator to produce neutron pulses having a width at half maximum of 3.9 μsec and a peak-to-minimum ratio of 12,400 by the rotation of a beryllium reflector (worth 4.8 dollars) past an unreflected core face 60 times/sec at a speed of 264 meters/sec. This pulse when thermalized by a 10.16 x 10.16 x 3.81 cm polyethylene scatterer is broadened to a width at half maximum of 20.9 μsec with a peak-to-minimum ratio of 1590. The use of cadmium distributed within the scatterer at 20°C can neither reduce the width of the pulse of low energy neutrons to less than 7 μsec nor increase the peak-to-minimum ratio to more than 7400.

The fraction of all neutrons that are in the pulse in the center of the core was 0.80 and was not a strong function of reactivity. This fraction was the same for the neutrons at the outer surface of the scatterer. All values measured at the different locations and reactivities were between 0.77 and 0.85.

The number of thermal neutrons leaking out the outer surface of the scatterer was 3.3×10^{-5} n/cm^2-fission. Thus, a repetitively pulsed booster of this type with 1/60 MW sec of energy in the pulse would produce $\sim 1.7 \times 10^{10}$ thermal neutrons/cm^2 per pulse with this scatterer.

The effective one-group fundamental mode decay constant (0.20 μsec^{-1}) which was obtained from the width of the neutron pulse in the core for the assembly with a maximum reactivity of +50 cents above delayed criticality was almost equal to half of the decay constant of the fast component of the prompt neutron decay (0.36 μsec^{-1}) for the delayed critical assembly with the rotor stationary. Simple one-group neutron kinetic theory was used to predict the fraction of neutrons in the pulse but the calculated values of the peak-to-average neutron density agreed with the experimental values only for the assembly with maximum reactivities of -5 and +26 cents. The use of this simple theory depended on realistic values of the effective normal mode decay constant which in this case were inferred from the experimental results.

APPENDIX A

CORE LOADING PATTERNS

Core Loading Pattern No.	Number of Fuel Rods	Location of Iron Rods[a]
1	85 1/4	1 thru 9 and 1st 1/2 and 4th 1/4 of No. 10
2	84 13/16	1 thru 9, 2nd 1/2 of No. 19, 1st 1/2 and top 3/16 of No. 10
3	84 3/4	1 thru 9, 2nd 1/2 of No. 19, 1st 1/2 and 4th 1/4 of No. 10
4	88 9/16	1, 2, 7, 8, 9, and 1st 1/2 and top 5/16 of No. 3
5	87 3/4	1, 2, 3, 7, 8, 9, and 1st 1/2 and 7th 1/8 of No. 6
6	88 5/8	1, 2, 7, 8, 9, and 1st 3/4 of No. 3
7	87 13/16	1, 2, 3, 7, 8, 9, and 1st 1/2 and 9th 1/16 of No. 6
8	87 11/16	1, 2, 3, 7, 8, 9, and 1st 9/16 and top 1/8 of No. 6
9	80 3/8	1 thru 12, 18, and 19
10	73 3/8	1 thru 20 and 21
11	77 3/8	1 thru 13, 16, 17, 18, and 19
12	88 1/2	1, 2, 7, 8, 9, and 1st 3/4 and top 1/8 of No. 3
13	85 7/8	1 thru 5, 7, 8, 9, and 2nd 1/2 of No. 19
14	83 7/8	1 thru 10 and 2nd 1/2 of No. 19
15	88 3/16	1, 2, 7, 8, 9, 1st 1/2 of No. 3, and 1st 9/16 and top 1/8 of No. 6
16	87 5/8	1, 2, 3, 7, 8, 9, and 1st 5/8 and top 1/8 of No. 6
17	86 1/4	1, 2, 3, 4, 6, 7, 8, 9, and top 1/8 of No. 5

a. All of the 95 holes in the core, designated by number in Fig. 1, were loaded with 24-cm-long iron and/or uranium rods. The diameter of the iron was 1.369 cm; of the uranium 1.379 cm. The linear density of the uranium was 27.87 g/cm. The fuel rods are divided into quarters numbered from the bottom up. The upper 5/8 of fuel rod location No. 58 did not contain uranium in order to accomodate a BF_3 proportional counter. Fuel rod location No. 60 contained a special uranium (648 g) rod with the thermocouples.

APPENDIX B

MECHANICAL TESTS WITH THE ROTATING BLADE ASSEMBLY AND INSPECTION OF ROTOR

In this Appendix the results of tests of the rotating assembly prior to performance of the repetitively pulsed experiments and the results of inspections of the rotor both before and after the experiments are presented. The total accumulated operating time for the rotor was 230 hours.

After careful dynamic balancing, early tests with air in the shroud showed that the heating rate of the air and the variations of the plane of rotation of the rotor were not satisfactory. Mechanical stability of the rotor was improved by providing a helium atmosphere in the shroud with a flow sufficient to maintain the pressure inside the shroud slightly above atmospheric. This flow was necessary since the shroud was not designed to be gas tight. Only 15 hp was necessary for equilibrium operation of the rotor in helium. After 12 sec the rotor attained its operating speed of 3596 rpm and after about 15 min it coasted to a complete stop after removal of power.

Capability for water cooling the periphery of the shroud was provided by soldering 1.27-cm-diam copper tubing to the shroud and then covering it with Thermon, a high thermal conductivity cement. The water flow of 4.5 gal/min in two parallel paths on each surface of the shroud (see Fig. B-1) was sufficient to maintain the helium temperature at 39°C.

The deflection of the rotor in an axial direction at the position of the beryllium insert was measured using an inductive type radio-frequency proximity gauge mounted in the shroud wall opposite the unreflected core face. A photograph of an oscilloscope trace of a signal from the gauge is shown in Fig. B-2. The gauge was located so that rotation of the rotor moved the beryllium insert past the senstive face of the gauge. The gauge, sensing only the distance to an object, produced a signal which essentially described the contour of the beryllium insert. A cross section of the rotor, through the center line of the beryllium, is shown for comparison in the lower part of Fig. B-2.

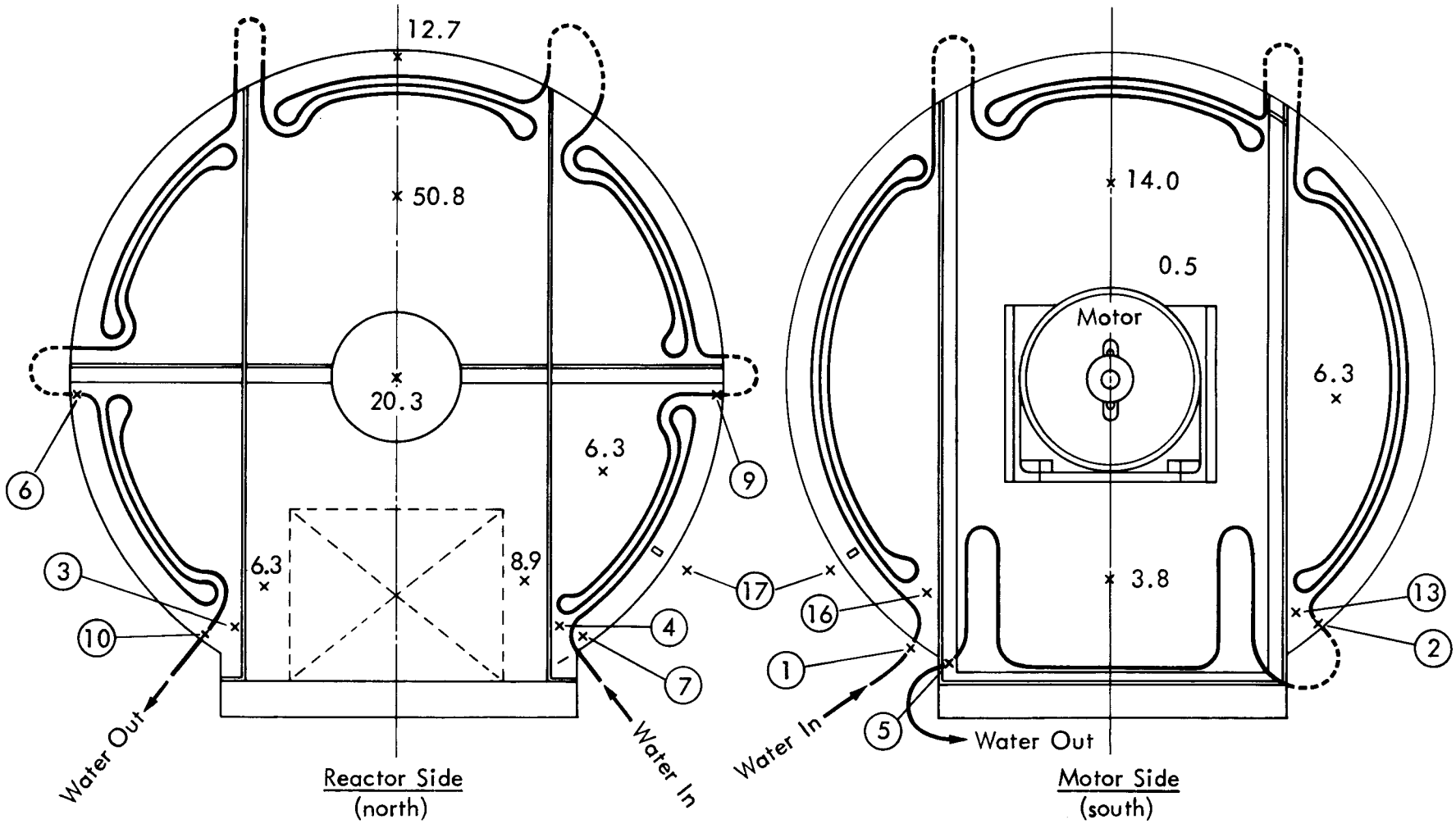

Fig. B-1. Sketches of the Shroud Enclosing the Rotor Showing the Locations of the Thermocouples and the Peak-to-Peak Vibrations Measured during Operation of the Rotor.

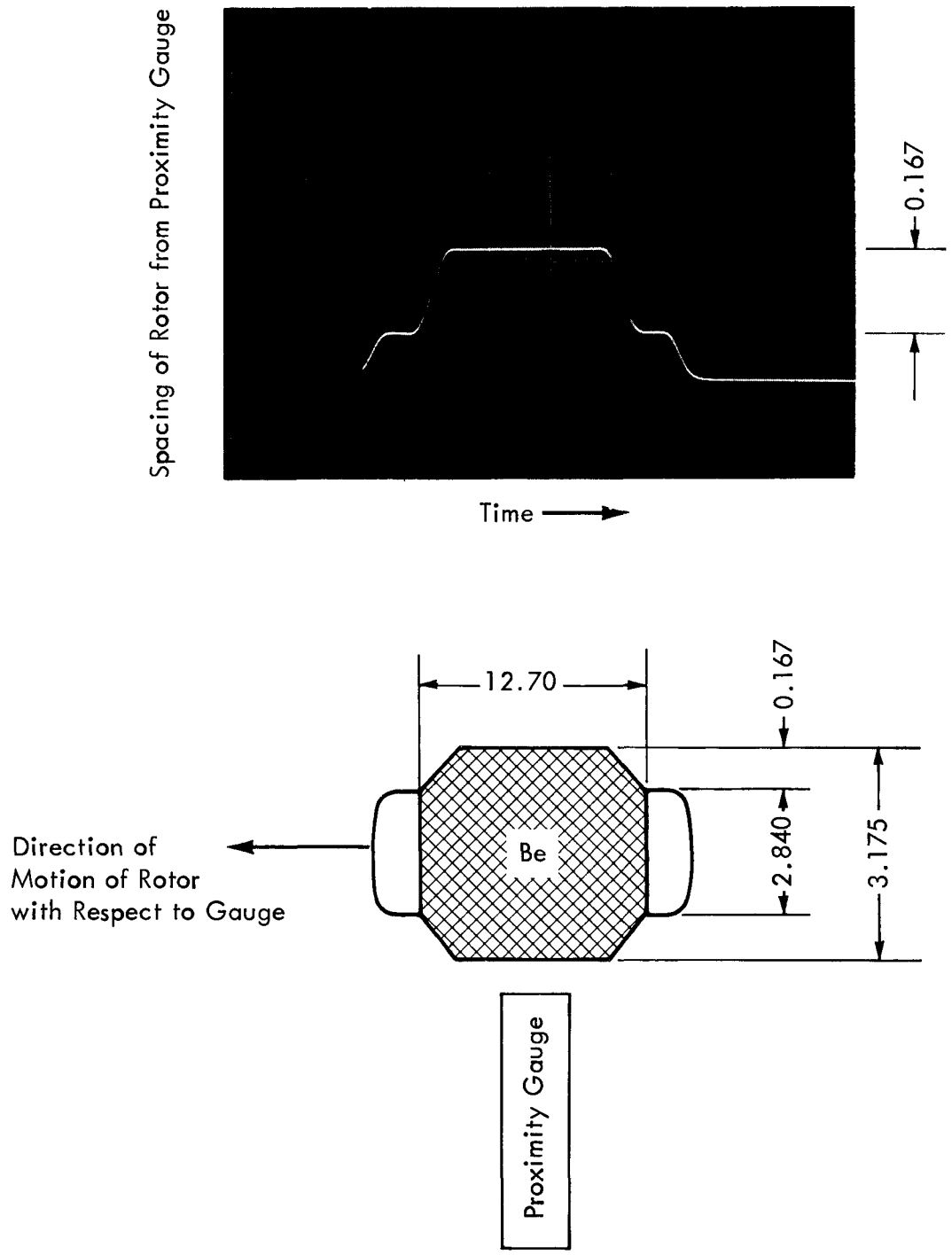

Fig. B-2. The Contour of the Beryllium Insert in the Rotor from the Proximity Gauge Displayed on an Oscilloscope.

The oscilloscope sweep was adjusted so that the entire 12.70 cm dimension was displayed. Figure B-3 shows the position of the beryllium with respect to the gauge mounted on the shroud when the rotor was proximate to the gauge during rotation at constant angular speed. That is, the horizontal oscilloscope time scale was adjusted so that each "dot" represents the upper horizontal trace in Fig. B-2. The eight rows of dots are successive exposures made so that many data, ~1040 revolutions in this case, were recorded on a single photograph. Deviation of the dots from the horizontal is a measure of the deviation of the beryllium surface from a fixed plane, perpendicular to the axis of rotation, during the test. From the sensitivity of the ordinate, 0.084 mm/cm, it was observed that the peak-to-peak variation of the plane of rotation, in the axial direction, was about 0.152 mm, total, or ±0.076 mm.

Figure B-4 shows, in a similar manner, the position of the beryllium with respect to the gauge following rapid shutdown (scram) of the assembly while the rotor was turning at constant angular speed. The shutdown, which occurred at zero time on the abscissa, consisted of dropping the core, by gravity, and rapidly displacing the largest section of the iron reflector (see Fig. 2) a distance of ~5 in. The distance between the beryllium of the rotor at the position of maximum reactivity and that part of the shroud adjacent to the unreflected core face decreased 0.102 mm during the first 0.5 sec following shutdown and then varied within ± 0.076 mm of the distance established during the steady operation described in Fig. B-2.

The peak-to-peak vibrations at various points on the shroud during operation of the rotor were measured with a commercially available accelorometer and the results are given in Fig. B-1. The vibration of the base of the core support stand with the motor running and the core inserted into the iron reflector was ± 0.051 mm and the value observed at the fixed iron reflector was less than 0.013 mm. These small vibrations did not cause reactivity changes of concern in the operation of the experiment.

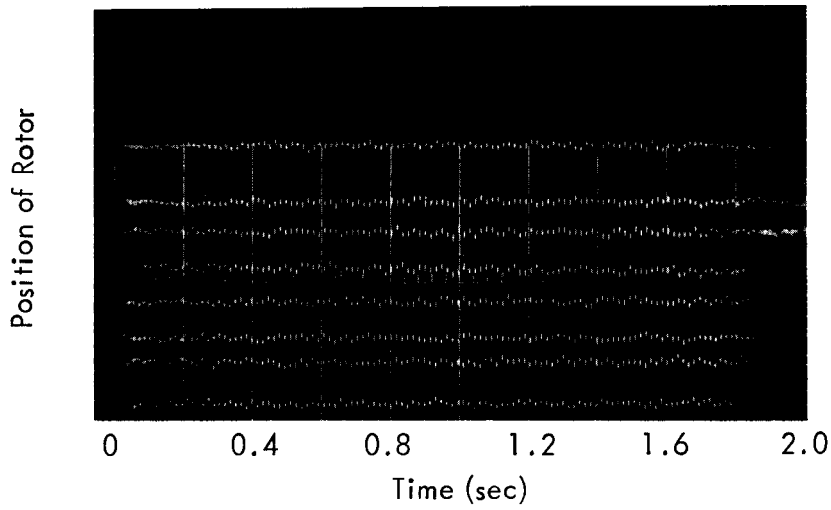

Fig. B-3. Variation in the Lateral Position of the Rotor during Uniform Rotation.

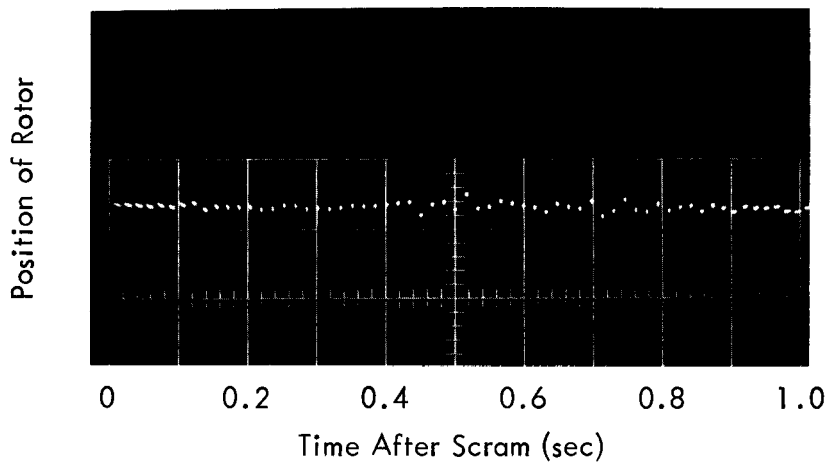

Fig. B-4. Variation in the Lateral Position of the Uniformly Rotating Rotor during Scram of the Assembly.

The location of the thermocouples for temperature measurements are also given in Fig. B-1 (numbers within circles). The temperatures observed during a 5.7 hr run are given in Table B-1. They indicate achievement of equilibrium at most locations within an hour. There was about a 3°C rise in the shroud-cooling water temperature when the supply was at 25°C. The equilibrium helium temperature was 39°C and the change in the temperature in the center of the core was about 8°C.

The rotor was initially inspected with liquid dye penetrant for indications of surface discontinuities and with ultrasound and X rays for internal discontinuities. None of these tests revealed any cracks, laminations, porosity, etc. that might significantly affect the structural strength of this assembly. Following operation of the rotor for ~27 hrs, it was again inspected by the same methods with no evidence of change in structural integrity. In addition, the 12 bolts were subjected to dye penetrant and X-ray inspection and no indication of significant defects was noted. Upon completion of the experiment, the rotor assembly was again inspected with dye penetrant, ultrasound, and X rays. The 12 bolts were subjected to dye penetrant and X-ray inspection also. No indication of significant defects or change from the initial inspection results was noted.

Table B-1. Temperature Measurements During a Typical Experiment.

Thermocouple No.	Location[a]	Temperature °C, Elapsed Time (min) 0	60	300	342
1	Water in	25	24	24	24
2	Water	25	26.2	27	27
3	Shroud	25.5	40	39.5	39.5
4	Shroud	26	36	36	36
5	Water out	25.5	29	29	28.5
7	Water in	25		23.5	23
10	Water out	25	27.5	27	27
13	Shroud	26	30	39.7	39.7
16	Shroud	25.5	35.2	35.2	35
17	in He	21.5	39	39	39
18	Core Center	25	27.5	33	33
--	Fe Reflector[b]	25	--	28	28

a. See Fig. B-1 for more detail.
b. Between the Boral and the iron reflector at midplane.

APPENDIX C

NEUTRON DECAY IN THE ISOLATED POLYETHYLENE SCATTERER

The time behavior of the neutrons leaking from the polyethylene scatterer, when isolated from the assembly, was measured by producing a pulse of 14.1 MeV neutrons with a 150 Kv Cockcroft-Walton accelerator adjacent to a 10.16 x 10.16 cm surface of the scatterer. The neutron distribution as a function of time was observed with a 0.79-cm-diam, 2.54-cm-long BF_3 proportional counter that was located at the center of the opposite 10.16 x 10.16 cm surface of the scatterer. The time behavior of all neutrons and of the epithermal neutrons, those with energies above the cadmium (0.063-cm-thick) cutoff energy, were measured. The function $A + B \exp(t)$ was fitted to the time behavior of the epithermal neutrons by least squares while the function $A + B \exp(\alpha_1 t) + C \exp(\alpha_2 t)$ was fitted to the time distribution of neutrons of all energies. The results of the fitting are shown with the data in Figs. C-1 and C-2. The differences between these decays and those presented for the polyethylene scatterer in the repetitively pulsed experiments were due to the broadening of the pulse by the core multiplication and to the effect of the motion of the rotating reflector.

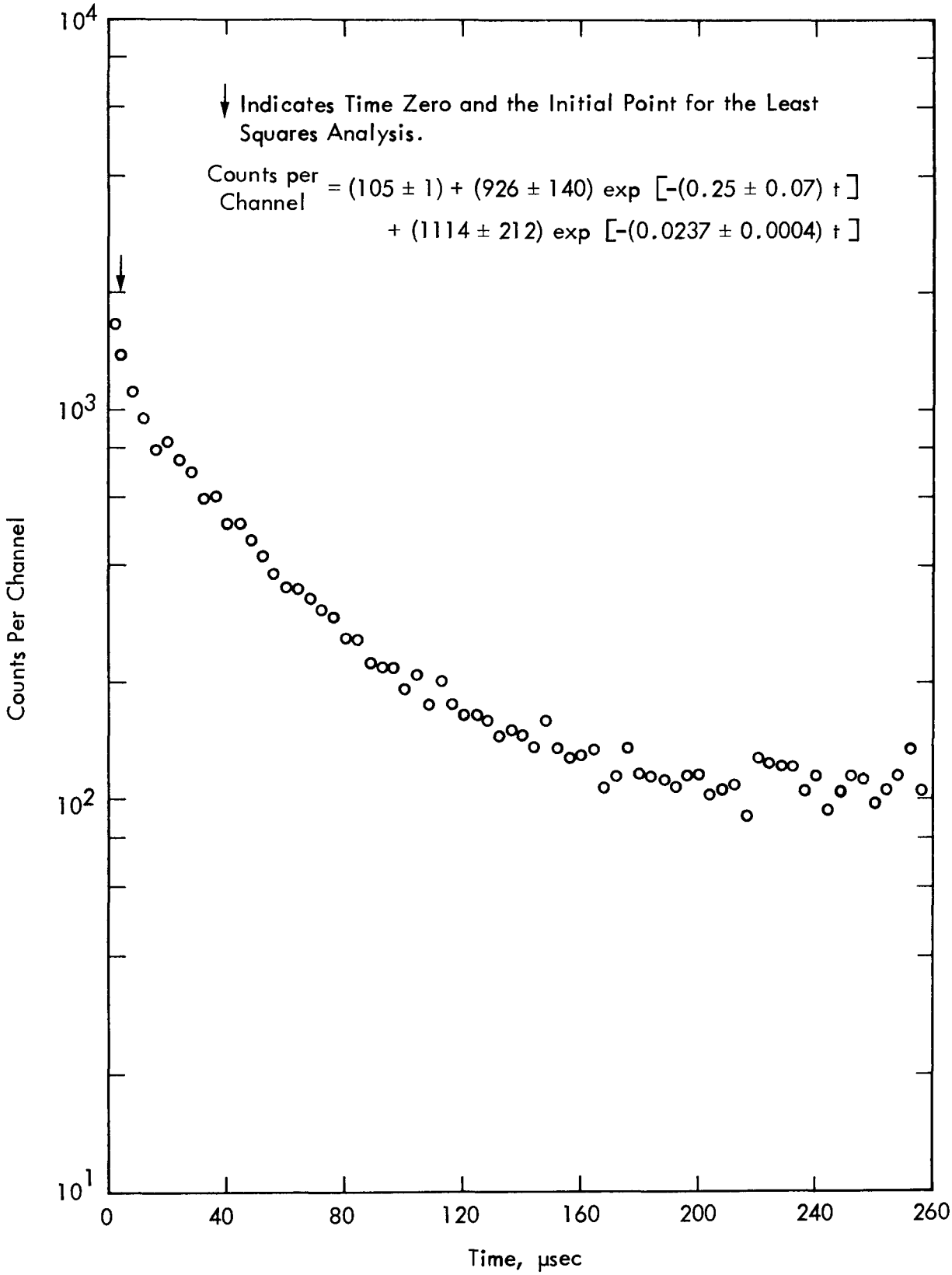

Fig. C-1. The Neutron Decay for the Isolated Polyethylene Scatterer.

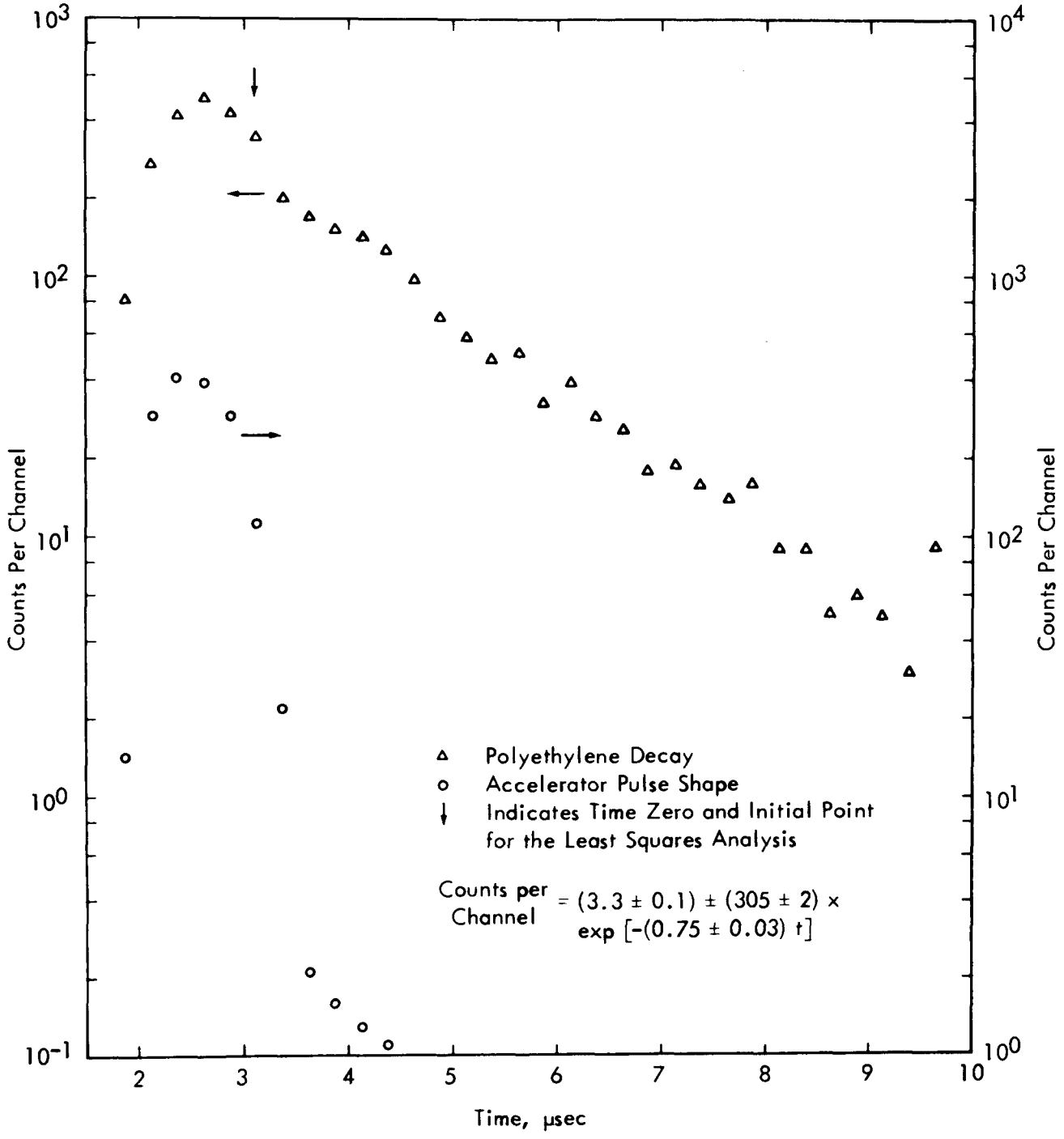

Fig. C-2. The Decay of Epithermal Neutrons for the Isolated Polyethylene Scatterer.

ACKNOWLEDGEMENTS

The author acknowledges the assistance of the staff of the Oak Ridge Critical Experiments Facility, in particular the work of J. J. Lynn and J. R Taylor in performance of the experiments and handling of the data and the work of E. R. Rohrer in electronic engineering. Acknowledgement is expressed to W. C. Tunnell for supervising and coordinating the design, construction, installation, and testing of the experimental assembly, particularly the rotating mechanism. Appreciation is expressed to J. F. Ellis for the development of the devices for monitoring the position of the rotating blade and for triggering the accelerator and the time analysis equipment.

Acknowledgement is expressed to Lloyd V. Wilson of Oak Ridge National Laboratory (ORNL) for the design and the balancing of the rotor. Appreciation is also expressed to V. H. Kiplinger of the Oak Ridge Gaseous Diffusion Plant (ORGDP) for his work in vibration analysis. Acknowledgement is expressed to R. Cuthbert, Jr.[a] of ORGDP for work in installation and testing at ORGDP. The author acknowledges the work of R. Rosenvinge of the Y-12 Plant for the design of the structure to enclose and support the rotating mechanism at the CEF.

The author is indebted to L. Weston, R. Gwin, and R. Ingle of ORNL for the use of the time interval counter and the PDP-4 computer and for the help of R. Ingle in the setup and use of this equipment. The author is grateful to F. Haywood of ORNL for the work in determining the thermal fluence at the scatterer and to E. I. Wyatt of ORNL for analysis of the fuel samples for fission product content.

[a]Now associated with the Oak Ridge Y-12 Plant.

DISTRIBUTION

Aktiebolaget Atomenergi--Sweden

Holmqvist, Bertel

Argonne National Laboratory

Redman, W. C.

Atomic Energy of Canada Limited

Tunnicliffe, P. R.
Westcott, C. H.

Atomic Energy Commission-ORO

DTIE (2)
Keller, C. A.
Lenhard, J. A.
Roth, H. M.
Zachry, D. S., Jr.

Atomic Energy Commission-Washington

Hannum, W. H.
Hemmig, P. B.
Legler, F. L.
Shon, F. J.

Atomic Energy Research Establishment Berkshire, England

Crocker, V. S.
Rae, E. R.

Atomic Weapons Research Establishment England

McTaggart, M. H.
Weale, J.

Ballistics Research Laboratory

Kazi, A. H.

Bariloche Atomic Center--Argentina

Antunez, H. M.

Bhabba Atomic Research Center, India

Nargundkar, V. R.

Brookhaven National Laboratory

Kouts, H. J. C.

Centre Etude Nuclaire--France

R. Joly

EURATOM-Ispra, Italy

Kley, W. (5)
Raievski, Victor

European Nuclear Energy--France

Smets, H. B.

Gulf General Atomic

Larrimore, J. A.
Preskitt, C. A.

Hoog Blok--Belgium

Spaepen, Josef

Idaho Nuclear Corporation

Brugger, R. M.
Morfitt, J. W.
Russell, G. J.

Institute fur Angelwandte Kernphysik--Germany

Beckurts, K. H.

Laboratorium fur Technische Physik-Munchen, Germany

Maier-Leibnitz, Heinz

Lawrence Radiation Laboratory

Kloverstrom, F. R.
Hampel, V. R.

Los Alamos Scientific Laboratory

Fluharty, R. G.
Moore, M. S.
Motz, H. T.
Paxton, H. C.
Williams, J. M.
Wimett, T. F.

Oak Ridge Gaseous Diffusion Plant

Barton, J. C.
Wilcox, W. J., Jr.

Oak Ridge National Laboratory

Affel, R. G.
Binford, F. T.
Culler, F. L.
de Saussure, G.
Harvey, J. A.
Jordan, W. H.
Laughon, K. (AEC)
Lundin, M. I.
Maienschein, F. C. (2)
Perry, A. M.

Oak Ridge Y-12 Plant

Burkhart, L. E.
Callihan, Dixon (10)
Johnson, E. B.
Magnuson, D. W.
Mihalczo, J. T. (10)
Strasser, G. A.
Strohecker, J. W.
Tunnell, W. C.
Googin, J. M.
Denny, A. (4)
Keith, Alvin
Mitchel, G. W.
Central Files (15)
Central Files (route)
Central Files (master copy)
Central Files (Y-12 RC)

Paducah Gaseous Diffusion Plant

Levin, R. W.

National Bureau of Standards

Penner, Sammuel

Rensselaer Polytechnic Institute

Block, R. C.
Gaerttner, E. R.

Sandia-Albuquerque

Coats, R. L.
Hasenkamp, A.

Savannah River Laboratory

Dessauer, G.

Science Applications

Beyster, J. R.

Tohoku University--Japan

Kimura, Mohoharu

University of Arizona

Hetrick, D. L.

University of Calif.--Berkeley

Pigford, T. H.

University of Cambridge--England

Frisch, O. R.

University of Florida

Uhrig, R. H.

University of Illinois

Adler, F. T.
Miley, G. H.

University of New Mexico

Long, R. L.

University of Saskatchwan--Canada

Katz, Leon

University of Toronto

McNeill, K. C.

White Sands Missile Range

De La Paz, Armando

Yale University

Schultz, G. J.